

Explosive Nucleosynthesis from GRB and Hypernova Progenitors: Direct Collapse versusFallback

Christopher L. Fryer^{1,2}, Patrick A. Young^{2,3}, Aimee L. Hungerford⁴

ABSTRACT

The collapsar engine behind long-duration gamma-ray bursts extracts the energy released from the rapid accretion of a collapsing star onto a stellar-massed black hole. In a collapsing star, this black hole can form in two ways: the direct collapse of the stellar core into a black hole and the delayed collapse of a black hole caused by fallback in a weak supernova explosion. In the case of a delayed-collapse black hole, the strong collapsar-driven explosion overtakes the weak supernova explosion before shock breakout, and it is very difficult to distinguish this black hole formation scenario from the direct collapse scenario. However, the delayed-collapse mechanism, with its double explosion, produces explosive nucleosynthetic yields that are very different from the direct collapse scenario. We present 1-dimensional studies of the nucleosynthetic yields from both black hole formation scenarios, deriving differences and trends in their nucleosynthetic yields.

Subject headings: Gamma Rays: Bursts, Nucleosynthesis, Stars: Supernovae: General

1. Introduction

Since the observation of SN 1997ef (Iwamoto et al. 2000), the number of strong supernovae has grown considerably. This class of supernova, termed hypernova, includes the supernovae associated with gamma-ray bursts (see Maeda & Nomoto 2003; Nomoto et al. 2004 for reviews). Indeed, one of the best observed examples of a hypernova is SN 1998bw,

¹Department of Physics, The University of Arizona, Tucson, AZ 85721

²Theoretical Division, LANL, Los Alamos, NM 87545

³Steward Observatory, The University of Arizona, Tucson, AZ 85721

⁴Computational and Computer Science Division, LANL, Los Alamos, NM 87545

which occurred concurrently and cospatially with Gamma-Ray Burst 980425 (Galama et al. 1998). It is believed that long-duration gamma-ray bursts (GRBs) make up a subset (perhaps even the entire set) of all hypernovae and it is often assumed that the engine driving all of these bursts is the same “collapsar” engine (Podsiadlowski et al. 2004).

The collapsar engine is powered by the gravitational energy released by matter accretion onto a stellar mass black hole, presumably from the collapse of a massive star (Woosley 1993). To extract this energy, this matter must hang up in a disk prior to moving into the event horizon of the black hole. Two mechanisms have been proposed to extract this accretion disk energy: neutrino annihilation and magnetic field eruptions (Narayan et al. 1992). This energy drives a strongly asymmetric explosion that develops into a strongly relativistic jet in the case of long-duration GRBs. Although the explosion is not strongly relativistic outside of the jet axis, it is likely that the entire star is disrupted by the explosion.

At the crux of this mechanism is the fact that the star collapses to a black hole. Stars can form black holes through two separate paths: the direct collapse of a star down to a black hole or the fallback of considerable material onto a proto-neutron star formed in a weak supernova explosion (Fryer 1999). Fryer & Kalogera (2001) argued that this latter scenario could well be the most common path behind black hole formation. Since the mechanisms (neutrino annihilation and magnetic fields) that extract the gravitational potential energy released in the disk do not require that the compact remnant be a black hole, it might be possible to produce hypernovae by accretion onto neutron stars if the rate of accretion is sufficiently high ($\gtrsim 0.1M_{\odot}s^{-1}$). In this paper, we will consider not only the direct and fallback collapse black-hole engines, but also these rapidly accreting neutron star scenarios.

Most of the current models for nucleosynthetic yields of hypernovae effectively assume that the black hole is formed in the direct collapse of a black hole (e.g. Nomoto et al. 2005a, 2005b and references therein). But with the possibility that a majority of hypernovae could be produced by fallback black-holes, we have a new paradigm for estimating the nucleosynthetic yields of these explosions. We will show in this paper that the nucleosynthetic yield from a single strong explosion is quite different from that of a weak supernova explosion followed by fallback and then a strong explosion. In §2, we show the results of our hypernova explosions and review the differences in the temperature and density evolution of ejecta for single strong explosions versus weak explosions followed after a range of delays by a strong explosion. In §3, we present the yields of these explosions. We conclude with a discussion of the primary trends in the yields, outlining the implications the yields have on hypernova progenitors and ultimately stellar collapse.

2. Hypernova Explosions

2.1. Numerical Setup and Single and Double Explosions

We focus our study on 2 potential hypernova progenitors: a $23 M_{\odot}$ star that loses its hydrogen envelope in a binary interaction prior to helium ignition (Case B mass transfer) and a $40 M_{\odot}$ single star (Young et al. 2006). Both observations (Hjorth et al. 2003; Stanek et al. 2003) and theoretical considerations (Woosley 1993; Zhang, Woosley, & MacFayden 2003) call for a progenitor with no hydrogen envelope. These progenitors represent the two primary formation channels for a hydrogen poor single star collapsar model (as opposed to a merger-induced GRB). We follow the evolution from collapse of the entire star through the bounce and stall of the shock using the 1-dimensional core-collapse code described in Herant et al.(1994) and Fryer et al. (1999). This code models the transport of 3 neutrino species ($\nu_e, \bar{\nu}_e, \nu_{\mu,\tau}$) using single energy flux-limited diffusion and takes advantage of a 4-part equation of state that covers a range of densities from above nuclear to ideal gas regimes and includes both a small nuclear network and nuclear statistical equilibrium prescriptions (see Herant et al. 1994 and Fryer et al. 1999 for details). At the end of this phase, the proto-neutron stars of the $23 M_{\odot}$ and $40 M_{\odot}$ stars have reached masses of $1.37 M_{\odot}$ and $1.85 M_{\odot}$, respectively.

At this point in the simulation, we remove the neutron star core and drive an explosion by artificially heating the 15 zones ($\sim 3 \times 10^{-2} M_{\odot}$) just above the proto-neutron star. The amount and duration of the heating is altered to achieve the desired explosion energy, where explosion energy is defined as the total final kinetic energy of the ejecta (see Table 1 for details). The neutron star is modeled as a hard surface. Figure 1 shows the velocity profiles of our strong explosions ($13, 14 \times 10^{51}$ erg for the $23, 40 M_{\odot}$ respectively). Note that the initial velocities are above $30,000 \text{ km s}^{-1}$ and even as the shock is breaking out of the star, the peak velocity is above $20,000 \text{ km s}^{-1}$ for both models. There is no fallback for these models. This explosion mimics the conditions for those gamma-ray bursts that are produced by the direct collapse of the star to a black hole.

The velocity profile of our weak supernova explosions ($0.25, 0.14 \times 10^{51}$ erg for the $23, 40 M_{\odot}$ respectively) is shown in Figure 2. Although the shock rises to peak velocities of $10,000 \text{ km s}^{-1}$, by the time the shock breaks out of the star, the peak velocities are less than $5,000\text{--}7,000 \text{ km s}^{-1}$. Notice also in Figure 1 that the inner material slows down as its energy is used to accelerate the material above it. This material decelerates below the escape velocity and falls back onto the neutron star. This is the primary mechanism for supernova fallback (see Fryer et al. 2006 for a review). As this material falls back onto the neutron star its density increases. When the density of a fallback zone rises above $5 \times 10^8 \text{ g cm}^{-3}$,

we assume that neutrino cooling will quickly cause this material to accrete onto the neutron star and we remove the zone from the calculation (adding its mass to the neutron star). The mass of the neutron star as a function of time is shown in Fig. 3. Be aware that even if no gamma-ray burst is produced, much of this material need not accrete onto the neutron star. Especially if this material has angular momentum, it is likely that some of it will be ejected in a second explosion. (In a case with no GRB this will presumably be due to a similar mechanism, but without the very high Lorentz factors.) This ejecta is a site of heavy element production (Fryer et al. 2006). As we focus here only on the explosive nucleosynthesis, we will not discuss this ejecta further.

The fallback black hole scenario corresponds to an initially weak explosion as is seen in Figure 2 that is then followed by a strong explosion. Without knowing the angular momenta of these stars (accurate angular momentum estimates are beyond the capability of current stellar evolution codes), it is difficult to determine when a disk will form that powers the collapsar engine. Hence, we consider a range of delay times corresponding to the onset of mass fallback onto the neutron star and to the timescale when the remnant mass exceeds 2 different limits (these limits are progenitor specific - see table 1). We produce the second explosion by taking the data from the weak explosion at a given time delay and then re-injecting energy into the base of the star (again, the inner $\sim 3 \times 10^{-2} M_{\odot}$) and driving an explosion with energy in excess of 10^{52} erg.

2.2. Second Temperature and Density Histories

The final nucleosynthetic yield of the ejected matter is set by the initial abundance (in particular the neutron excess), but even more importantly by the density and temperature evolution of the ejecta. We must understand this evolution before we can understand the final yields of these explosions. Figure 4 shows the temperature evolution of 2 mass zones in our explosion models. Figure 5 shows the density evolution for these same zones. Note that the structure changes dramatically for the different explosion models.

The behavior in these figures can easily be understood by using shock jump conditions to determine the density (ρ_{shock}) and pressure (P_{shock}) after the shock has passed (e.g. Chevalier 1989):

$$\rho_{\text{shock}} = \frac{(\gamma + 1)M^2}{(\gamma - 1)M^2 + 2}\rho_0 \quad (1)$$

$$P_{\text{shock}} = (2\rho_0 v_{\text{shock}}^2 - (\gamma - 1)P_0)/(\gamma + 1) \quad (2)$$

where γ is the adiabatic, M and v_{shock} are the Mach number and velocity respectively of the shock, and ρ_0, P_0 are the initial density and pressure profiles. In the strong shock limit,

these equations reduce to familiar limits:

$$\rho_{\text{shock}} = (\gamma + 1)/(\gamma - 1) \rho_0 \quad (3)$$

$$P_{\text{shock}} = (2\rho_0 v_{\text{shock}}^2)/(\gamma + 1). \quad (4)$$

In the strong shock limit we expect the pressure, and hence the temperature, to depend upon the velocity of the shock, but the density is increased by a constant factor (independent of the shock velocity). When not in the strict strong shock regime, the density jump will be slightly less than $(\gamma + 1)/(\gamma - 1)$. The temperature is a function of the pressure (e.g. $P^{1/4}$ for a radiation dominated gas).

Figure 4 shows the temperature evolution of two different zones for all 10 explosion simulations: Fig. 4a,4b show the results of the $23 M_\odot$ binary, $40 M_\odot$ progenitors respectively. The rightmost panel shows the temperature evolution of two mass zones for our strong explosion. When the shock hits the matter, its temperature increases abruptly as we expect from our shock jump conditions. Material further out reaches lower peak temperatures. The leftmost panel shows the same mass zones in our weak explosion. Because the explosion is weaker, the peak temperature is much lower. The middle 3 panels show the evolution of our weak plus strong explosions with the total delay decreasing as we move from left to right. If the delay is long, the matter expands so much after the first weak explosion that the second explosion is unable to heat the material significantly. As the delay shortens, the peak temperature approaches that of the single strong shock. This peak temperature plays a crucial role in determining the nucleosynthetic yield. Recall that the total energy in all the weak+strong and the strong explosions are nearly identical. So although the energetics of the explosions will all appear identical, their yields will be quite different.

Figure 5 shows the corresponding density evolution of all our simulations. Note the near constant density jump for the weak and strong explosions. The slight difference in density jump occurs because we are approaching, not at, the strong shock limit. In general for the weak+strong shock models, the material expands considerably after the first shock and its density after the strong shock hits is increased, but not higher than its peak value. The exceptions are the short delays, for which the peak density can be higher than what would be obtained from a single strong explosion.

3. Nucleosynthetic Yields

The nucleosynthetic yield of the ejecta is determined by the initial abundance and the temperature, density, and electron (or neutron) fraction evolution. The small nuclear network used in the simulation itself assumes a fixed neutron excess. We then post-process

the ejecta in our hydrodynamical explosions using a 524 element nuclear network. The initial abundance is set by the stellar models (again, see Young et al. 2006), which also sets the electron fraction we use for the hydro simulations. For our models, which leave behind large remnants, the initial electron fraction is between 0.497 and 0.5.

Figure 6 shows the nickel, titanium, silicon, oxygen, and carbon mass fraction profiles of our ejecta as a function of enclosed mass. Actually predicting the yields of our complex temperature and density evolutionary tracks is very difficult, but we can predict some trends based on the fact that the peak temperature for a piece of matter decreases for longer delays in the explosion, first and foremost being that nuclear burning should be less and we should expect a lower production rate of the heavier explosive elements like ^{56}Ni and ^{44}Ti . This trend is compounded by the fact that, for longer delays, more material falls back and less inner material (material that typically forms these heavy elements) is ejected. And indeed, this is the trend we see in our simulations - longer delays in the explosion produce less ^{56}Ni and ^{44}Ti .

The detailed yields of all our elements heavier than hydrogen are listed in tables 2 and 3. Beyond the fact that the weak plus strong explosions with long delays produce much less ^{56}Ni and ^{44}Ti , we highlight just a few other features of these models. First off, although there are mass elements in the star that produce high ^{44}Ti to ^{56}Ni , the composite yields lead to ratios of ^{44}Ti to ^{56}Ni that are generally lower than the solar abundance ratio of the stable daughter products of these elements: ^{44}Ca to ^{56}Fe .

As with Maeda & Nomoto (2003), we find the production of $A \gtrsim 60$ elements (e.g. ^{64}Zn and ^{59}Co) is high relative to iron. In the case of our 23 M_\odot models, the ratio of $^{64}\text{Zn}/^{56}\text{Fe}$ can be 10 times solar. In general, the ratio decreases with longer delays. The enhanced production of these elements is not so extreme in our 40 M_\odot models, and the difference between stellar progenitor are much greater than the differences caused by our different explosion scenarios. Such abundances are hence better suited to differentiated progenitors, and not the delay in the explosion model.

We also specifically studied the production sites of calcium and titanium. Figure 7 shows the abundance fraction of stable calcium and titanium as a function of enclosed mass for 4 models: 23strong, 23WS1.0, 40Strong, 40WS4.8. On average, the iron is most centrally concentrated with the mean of the titanium further out, and the mean of the calcium production even further out. But these regions all overlap. For the long delays, it appears that the distributions of all the elements are more centrally located.

A few other points are worthy of note in the nucleosynthesis. Material initially at roughly the neutron excess of the solar Fe peak can end up in the ejecta, especially if we include

explosions from rapid accretion onto neutron stars. In addition, delays of seconds after a weak explosion can result in matter remaining at high density long enough for weak interactions to operate and increase the neutron excess before the strong shock passes through. In the strong explosions and short delay weak+strong explosions the peak temperatures are very high. In most regions, the material is dissociated into α particles and then burned back up into the heavy element abundances we observe. In the innermost regions of these explosions the radiation entropy $S_R > 1.0 \times 10^8$, and the material is dissociated into proton and neutrons before burning back. This material is a small fraction of the star and so plays little role in the observed yields but exhibits interesting nuclear physics. Note also that nearly all of the helium in all of our models (except our single weak explosions) is burned into heavier elements (mostly carbon and oxygen). Even though these stars collapsed as helium stars, the strong explosions would make them appear to be helium poor stars.

Lastly, we show the velocity histogram of the different elements for a few of our explosions. The nickel and titanium velocity profiles are much more narrow than the silicon, carbon, and oxygen profiles. However, the velocities are all high (as we would expect from our $13\text{--}14 \times 10^{51}$ erg explosions). These velocity profiles are probably not a good representation of hypernova velocity profiles, which are strongly affected by the asymmetries in the explosions.

4. Conclusion

A collapsing star can form black holes in two ways: a direct collapse with no supernova explosion or the delayed collapse caused by fallback accretion after a weak supernova explosion. The collapsar engine for gamma-ray bursts and hypernovae can work using either of these black hole formation mechanisms. We have found in this paper that the nucleosynthetic yields of these two mechanisms, if dominated by explosive nucleosynthesis, will be quite different. These differences can be used to distinguish the black hole formation scenario, and ultimately, the progenitors of these outbursts. We have focused on the ^{56}Ni yield. For direct collapse black holes, or black holes formed shortly (< 1 s) after a weak explosion, the nickel yield tends to be much higher than the yield produced by black holes formed after a considerable delay (> 1 s). Hypernovae with high nickel yields (e.g. SN 1998bw) argue for short delays or direct collapse.

There are a number of effects that can flatten out this trend. Explosions are asymmetric and the asymmetries may lead to a lower nickel yield in the strong explosions. Also the disk itself may contribute significantly to the nickel yield by driving winds producing more nickel in the explosions with long delays. The yield also depends sensitively on the exact

progenitor. But we suspect these complexities will not completely wash out the basic trend of the decreasing nickel production with an increase in the delay between weak and strong explosion. Especially near the $20 M_{\odot}$ progenitor limit, we see a range of nickel yields in supernovae: compare the $0.32 M_{\odot}$ of ^{56}Ni predicted for SN2005bf (Tominaga et al. 2005) against the $\sim 4 M_{\odot}$ of ^{56}Ni in SN1999as (Deng et al. 2001).

We also notice that for our particular progenitors, the stars are sufficiently compact and the hypernova explosion energies are so large that, even though these stars collapse as helium stars, their helium is almost completely burned into heavier elements. So a helium-rich star (technically believed to be a Type Ib progenitor) can explode as a helium-poor star (or Type Ic supernova). Again, asymmetric explosions and different progenitors can alter this result, but it suggests that possibly the fact that most hypernovae appear to be type Ic supernovae may not mean that the progenitor star has lost most of its helium envelope at collapse.

Acknowledgments We would like to thank many useful conservations with Dave Arnett, Paolo Mazzali, Ken Nomoto, and Kei’ichi Maeda. This work was funded in part under the auspices of the U.S. Dept. of Energy, and supported by its contract W-7405-ENG-36 to Los Alamos National Laboratory, by a DOE SciDAC grant DE-FC02-01ER41176, a NASA grant SWIF03-0047, and by National Science Foundation under Grant No. PHY99-07949.

REFERENCES

- Chevalier, R.A. 1989, ApJ, 346, 847
- Deng, J.S., Hatano, K., Nakamura, T., Maeda, K., Nomoto, K., Nugent, P., Aldering, G., & Branch, D. 2001, ASP Conf. Proc. 251, p. 238, eds. H. Inoue & H. Kuniewda, ASP (San Francisco)
- Fryer, C.L. 1999, ApJ, 522, 413
- Fryer, C.L., Benz, W., Herant, M., & Colgate, S.A. 1999, ApJ, 516, 892
- Fryer, C.L. & Kalogera, V., ApJ, 554, 548
- Fryer, C.L., Herwig, F., Hungerford, A.L., & Timmes, F.X. 2006, submitted to ApJL
- Galama, T. J., et al. 1998, Nature, 395, 670
- Herant, M., Benz, W., Hix, W.R., Fryer, C.L., & Colgate, S.A. 1994, ApJ, 435, 339
- Hjorth, J. et al. 2003, Nature, 423, 897

- Iwamoto, K., Nakamura, T., Nomoto, K., Mazzali, P.A., Danziger, I.J., Garnavich, P., Kirshner, R., Jha, S., Balam, D. & Thorstensen, J. 2000, ApJ, 534, 660
- Maeda, K. & Nomoto, K. 2003, ApJ, 598, 1163
- Narayan, R., Paczynski, B., & Piran, T. 1992, ApJ, 395, L83
- Nomoto, K., Maeda, K., Mazzali, P.A., Umeda, H., Deng, J., & Iwamoto, K., in “Stellar Collapse”, Astroph. & Space Science Library, ed. Chris Fryer, Kluwer Academic Publishers (Dordrecht)
- Nomoto, K., Maeda, K., Tominaga, N., Ohkubo, T., Deng, J. & Mazzali, P. A. 2005, Ap&SS, 298, 81
- Nomoto, K., Tominaga, N., Umeda, H., Maeda, K., Ohkubo, T., & Deng, J. 2005, Ap&SS, 298, 81
- Podsiadlowski, P., Mazzali, P.A., Nomoto, K., Lazzati, D., & Capellaro, E. 2004, ApJ, 607, L17
- Stanek, K. Z., et al. 2003, ApJ, 591, L17
- Tominaga et al. 2005, ApJ, 733, L97
- Woosley, S. 1993, ApJ, 405, 273
- Young, P.A., Fryer, C.L., Hungerford, A., Arnett, D., Rockefeller, G., Timmes, F.X., Voit, B., Meakin, C., & Eriksen, K.A. 2006, accepted by ApJ
- Zhang, W., Woosley, S. E. & MacFayden, A. I. 2003, ApJ, 585, 356

Table 1. Explosion Models

Model Name	$t_{\text{delay}}^{\text{a}}$ (s)	\dot{E}^{b} (10^{54} erg s $^{-1}$)	$t_{\text{Heating}}^{\text{c}}$ (ms)	$E_{\text{Explosion}}^{\text{d}}$ (10^{51} erg)	$M_{\text{Remnant}}^{\text{e}}$ (M $_{\odot}$)
23Weak	0	1	4	0.25	2.1
23WS0.7	0.7 ^f	8	3	15	1.4
23WS1.0	1.0 ^f	8	3	15	1.6
23WS2.6	2.6 ^f	8	5	16	1.8
23Strong	0	8	4	14	1.4
40Weak	0	2	24	0.1	6.3
40WS1.0	1.0 ^f	15	15	16	2.4
40WS4.8	4.8 ^f	15	16	16	3.0
40WS6.8	6.8 ^f	15	19	17	3.2
40Strong	0	15	24	13	2.4

^aDelay between the beginning of simulation and the time we begin to deposit energy.

^bEnergy deposited in the inner 15 zones of the simulation. For the delayed explosions, we use the heating rate for the weak explosion and then, after a delay, add the heating rate listed in the table.

^cTime that we deposit the energy.

^dTotal kinetic energy in the explosion when the shock hits the edge of the star.

^eMass of material that will not escape the gravitational potential well of the remnant. Some of this material is still moving outward at the end of the simulation, but its velocity is less than the escape velocity.

^fThe delay times for the 23 M $_{\odot}$ models correspond to the onset of accretion (23WS0.7), a 1.6 M $_{\odot}$ remnant (23WS1.0), and a 1.7 M $_{\odot}$ remnant (23WS2.6). The delay times for the 40 M $_{\odot}$ models corre-

spond to an early explosion at 1.0s (40WS1.0), the onset of accretion (40WS4.8), and a $2.6 M_{\odot}$ remnant (23WS2.6).

Table 2. Detailed Yields (M_{\odot}) Before Decay of Radioactive Species for $40 M_{\odot}$ Progenitor

Species	Weak	WS6.8s	WS4.8s	WS1.0s	Strong
^3He	2.36E-25	1.00E-17	4.92E-17	3.21E-15	1.56E-15
^4He	4.59E-03	3.16E-02	7.27E-02	1.28E-02	8.97E-02
^6Li	3.15E-21	1.78E-19	1.69E-19	1.91E-19	1.88E-19
^7Li	1.51E-25	1.79E-21	4.57E-21	1.23E-20	7.01E-21
^7Be	6.76E-24	9.14E-21	8.90E-21	8.45E-21	6.26E-21
^8Be	1.93E-25	1.99E-06	1.35E-06	1.20E-06	2.41E-06
^9Be	1.66E-23	1.60E-21	7.94E-22	6.28E-22	2.25E-22
^8B	1.52E-41	1.17E-33	7.96E-34	1.81E-36	2.08E-38
^{10}B	3.92E-20	1.21E-19	1.85E-19	2.42E-19	4.37E-19
^{11}B	8.76E-25	1.49E-12	2.14E-12	1.82E-13	1.91E-13
^{11}C	1.88E-23	1.92E-17	2.31E-17	2.71E-17	1.19E-17
^{12}C	1.39E-01	5.00E-01	5.13E-01	3.79E-01	3.89E-01
^{13}C	5.32E-09	4.80E-06	5.26E-06	1.19E-06	1.29E-06
^{14}C	1.08E-12	8.33E-07	1.30E-06	3.71E-07	2.81E-07
^{12}N	2.74E-36	8.20E-31	1.17E-30	1.47E-31	2.25E-34
^{13}N	8.56E-09	7.80E-08	1.01E-07	1.18E-07	1.22E-07
^{14}N	1.15E-12	7.76E-07	1.19E-06	7.60E-07	3.59E-07
^{15}N	8.91E-14	1.04E-07	1.46E-07	7.74E-08	7.81E-08
^{14}O	2.14E-15	8.57E-12	1.26E-11	1.54E-12	1.39E-12
^{15}O	9.64E-19	7.79E-11	9.43E-11	3.12E-10	1.20E-10
^{16}O	6.63E-01	3.43E+00	3.60E+00	3.24E+00	2.66E+00
^{17}O	4.72E-09	4.65E-07	4.82E-07	1.74E-07	1.67E-07
^{18}O	1.83E-11	1.14E-07	9.86E-08	7.40E-08	7.31E-08
^{19}O	1.09E-17	4.58E-12	1.83E-12	2.07E-12	2.00E-12
^{17}F	3.04E-14	4.82E-15	5.20E-15	6.73E-15	8.72E-15
^{18}F	6.16E-14	3.16E-09	3.68E-09	6.57E-09	2.74E-09
^{19}F	4.28E-10	3.17E-08	3.96E-08	2.69E-08	2.78E-08
^{20}F	1.17E-14	1.08E-09	1.45E-09	7.33E-10	7.04E-10
^{21}F	1.88E-19	1.15E-11	1.97E-11	3.33E-11	1.94E-11
^{17}Ne	1.43E-64	1.05E-37	9.60E-40	4.06E-41	1.24E-41
^{18}Ne	5.79E-23	1.25E-16	1.49E-16	1.76E-18	5.04E-19

Table 2—Continued

Species	Weak	WS6.8s	WS4.8s	WS1.0s	Strong
¹⁹ Ne	6.37E-21	1.86E-14	3.48E-14	1.59E-13	4.34E-14
²⁰ Ne	4.63E-02	1.80E-01	1.77E-01	1.71E-01	1.61E-01
²¹ Ne	2.62E-04	1.29E-03	1.31E-03	1.07E-03	1.11E-03
²² Ne	9.24E-03	3.46E-02	3.44E-02	2.24E-02	2.41E-02
²³ Ne	9.94E-09	2.36E-05	2.39E-05	1.75E-05	1.69E-05
²⁴ Ne	1.39E-15	1.80E-09	2.11E-09	1.24E-09	1.20E-09
¹⁹ Na	1.25E-45	3.94E-31	1.74E-31	9.07E-35	4.07E-40
²⁰ Na	3.42E-32	2.56E-18	4.89E-18	7.17E-21	8.19E-23
²¹ Na	1.22E-11	5.24E-09	7.42E-09	7.91E-09	7.43E-09
²² Na	2.72E-08	6.54E-07	1.32E-06	1.23E-06	9.97E-07
²³ Na	6.09E-04	3.13E-03	3.56E-03	2.08E-03	1.98E-03
²⁴ Na	1.39E-08	3.56E-05	4.39E-05	1.91E-05	1.93E-05
²⁵ Na	3.10E-13	3.28E-07	4.45E-07	1.74E-07	1.72E-07
²⁶ Na	1.48E-19	1.97E-10	1.85E-10	4.41E-11	2.90E-11
²⁷ Na	3.85E-27	2.09E-14	5.83E-15	4.44E-16	1.25E-16
²⁰ Mg	2.14E-60	3.69E-37	5.85E-38	1.60E-42	2.50E-51
²¹ Mg	2.19E-43	7.35E-21	6.30E-21	3.61E-25	2.04E-31
²² Mg	9.57E-19	8.19E-11	1.25E-10	1.46E-12	2.00E-14
²³ Mg	1.51E-15	3.27E-06	5.21E-06	1.15E-05	6.15E-06
²⁴ Mg	3.15E-03	4.05E-02	4.70E-02	4.19E-02	2.82E-02
²⁵ Mg	9.72E-04	6.94E-03	7.06E-03	5.10E-03	4.34E-03
²⁶ Mg	2.19E-03	1.11E-02	1.12E-02	7.63E-03	6.72E-03
²⁷ Mg	1.11E-09	5.80E-06	7.10E-06	3.20E-06	3.07E-06
²⁸ Mg	2.75E-14	5.87E-08	8.21E-08	3.00E-08	2.95E-08
²⁹ Mg	6.28E-21	7.88E-12	1.22E-12	1.43E-12	9.81E-13
²² Al	2.67E-72	8.31E-39	1.97E-39	7.12E-47	2.42E-57
²³ Al	1.60E-36	1.06E-22	1.04E-22	2.48E-24	2.07E-32
²⁴ Al	5.18E-24	1.39E-14	3.22E-14	2.93E-16	2.03E-18
²⁵ Al	2.69E-10	1.65E-07	3.54E-07	2.02E-08	1.71E-08
²⁶ Al	1.44E-09	9.83E-06	1.40E-05	1.38E-05	6.73E-06
²⁷ Al	1.09E-04	1.52E-03	1.56E-03	1.77E-03	8.32E-04

Table 2—Continued

Species	Weak	WS6.8s	WS4.8s	WS1.0s	Strong
^{28}Al	2.47E-09	5.01E-05	4.31E-05	1.72E-05	1.05E-05
^{29}Al	1.73E-13	1.30E-06	1.27E-06	2.69E-07	2.30E-07
^{30}Al	8.35E-19	1.42E-09	2.28E-09	4.39E-10	3.90E-10
^{31}Al	1.59E-24	2.25E-12	3.84E-12	3.96E-13	2.77E-13
^{23}Si	2.15E-91	9.25E-49	7.60E-50	5.93E-59	1.67E-72
^{24}Si	1.24E-45	1.27E-23	5.44E-24	9.85E-27	1.37E-29
^{25}Si	2.31E-34	6.14E-16	7.02E-16	2.23E-19	4.02E-27
^{26}Si	1.34E-18	5.13E-09	8.88E-09	1.36E-10	4.36E-11
^{27}Si	5.56E-16	4.06E-07	8.04E-07	2.94E-06	1.59E-06
^{28}Si	6.35E-04	7.16E-02	1.24E-01	5.32E-01	4.65E-01
^{29}Si	7.03E-05	3.74E-03	4.72E-03	5.71E-03	2.46E-03
^{30}Si	2.77E-05	6.07E-03	8.12E-03	8.25E-03	4.62E-03
^{31}Si	1.06E-09	2.86E-05	3.26E-05	2.52E-05	9.29E-06
^{32}Si	3.40E-11	1.39E-06	1.91E-06	4.78E-07	1.60E-07
^{33}Si	4.43E-17	9.67E-11	1.77E-10	5.04E-11	4.55E-11
^{34}Si	1.40E-22	1.14E-13	2.91E-13	5.32E-14	4.40E-14
^{27}P	3.43E-32	2.79E-16	5.20E-16	1.82E-17	1.03E-24
^{28}P	9.17E-27	8.17E-12	1.06E-11	1.54E-14	4.55E-19
^{29}P	5.60E-13	1.92E-07	3.03E-07	4.05E-09	2.36E-07
^{30}P	1.01E-11	7.71E-07	1.57E-06	9.47E-06	4.24E-06
^{31}P	7.62E-06	6.50E-04	8.81E-04	1.70E-03	8.72E-04
^{32}P	4.14E-09	7.55E-06	9.17E-06	5.45E-06	2.17E-06
^{33}P	4.57E-09	9.57E-06	1.27E-05	6.27E-06	4.62E-06
^{34}P	5.41E-14	4.52E-08	6.85E-08	1.73E-08	1.50E-08
^{35}P	2.51E-18	1.61E-09	2.17E-09	2.63E-10	2.98E-10
^{36}P	3.95E-24	1.06E-14	4.58E-15	3.75E-15	3.63E-15
^{37}P	3.72E-30	9.36E-17	7.42E-17	9.87E-18	6.16E-18
^{38}P	4.09E-39	1.04E-22	2.04E-24	3.92E-25	5.26E-26
^{28}S	1.60E-48	4.34E-25	2.01E-25	2.63E-27	6.99E-26
^{29}S	5.11E-38	1.15E-15	7.92E-16	3.62E-19	9.48E-25
^{30}S	6.48E-22	8.23E-09	5.59E-09	2.66E-10	2.82E-08

Table 2—Continued

Species	Weak	WS6.8s	WS4.8s	WS1.0s	Strong
^{31}S	1.43E-19	1.79E-07	1.43E-07	3.01E-07	2.19E-07
^{32}S	3.22E-04	3.52E-02	5.53E-02	2.77E-01	2.50E-01
^{33}S	1.84E-05	1.75E-04	2.25E-04	6.54E-04	4.41E-04
^{34}S	1.63E-05	3.03E-03	4.13E-03	1.49E-02	9.33E-03
^{35}S	5.96E-08	7.17E-06	9.12E-06	1.59E-05	7.44E-06
^{36}S	8.81E-08	1.19E-05	1.59E-05	1.58E-05	6.41E-06
^{37}S	1.59E-13	2.46E-09	2.47E-09	1.36E-09	1.33E-09
^{38}S	1.99E-18	1.18E-11	2.44E-11	8.03E-12	7.62E-12
^{39}S	9.28E-24	2.27E-14	4.49E-14	1.15E-14	1.08E-14
^{40}S	1.34E-28	1.10E-16	4.11E-16	6.80E-17	6.09E-17
^{41}S	9.60E-36	1.02E-20	2.97E-21	7.00E-22	4.35E-22
^{42}S	1.23E-40	3.61E-23	1.54E-22	1.08E-23	8.01E-24
^{31}Cl	7.43E-38	1.04E-19	3.17E-20	2.01E-20	2.48E-23
^{32}Cl	1.04E-30	6.72E-12	2.76E-12	2.67E-14	5.93E-18
^{33}Cl	4.54E-13	4.89E-07	1.62E-06	1.63E-08	4.62E-08
^{34}Cl	1.30E-14	7.89E-08	1.33E-07	1.20E-07	2.36E-06
^{35}Cl	4.04E-06	4.29E-05	4.99E-05	3.78E-04	2.63E-04
^{36}Cl	1.58E-07	1.39E-06	1.80E-06	3.01E-06	1.89E-06
^{37}Cl	4.42E-06	3.45E-05	3.90E-05	2.85E-05	2.33E-05
^{38}Cl	5.71E-11	5.01E-07	5.96E-07	2.69E-07	2.48E-07
^{39}Cl	7.67E-15	8.43E-08	9.57E-08	2.15E-08	1.65E-08
^{40}Cl	2.41E-19	6.57E-10	8.25E-10	1.90E-10	1.71E-10
^{41}Cl	2.25E-23	1.91E-10	1.94E-10	1.93E-11	1.04E-11
^{42}Cl	4.56E-28	4.03E-13	5.54E-13	6.54E-14	5.03E-14
^{43}Cl	1.72E-32	1.05E-13	9.08E-14	4.12E-15	1.67E-15
^{44}Cl	1.04E-39	6.64E-20	3.89E-20	3.50E-21	1.89E-21
^{45}Cl	8.64E-44	8.69E-22	6.30E-21	3.09E-22	2.20E-22
^{32}Ar	1.62E-53	3.17E-24	5.48E-25	6.83E-26	3.62E-22
^{33}Ar	7.41E-43	2.27E-16	3.98E-17	7.92E-20	6.59E-21
^{34}Ar	3.19E-22	1.82E-08	2.73E-08	5.05E-10	2.36E-07
^{35}Ar	2.42E-22	6.10E-08	3.83E-08	1.01E-08	3.31E-07

Table 2—Continued

Species	Weak	WS6.8s	WS4.8s	WS1.0s	Strong
^{36}Ar	7.35E-05	6.75E-03	9.08E-03	4.63E-02	4.55E-02
^{37}Ar	7.19E-07	1.10E-05	1.38E-05	7.02E-05	4.02E-05
^{38}Ar	1.50E-05	1.58E-03	1.98E-03	1.13E-02	5.76E-03
^{39}Ar	3.24E-07	3.58E-06	4.21E-06	2.48E-06	2.13E-06
^{40}Ar	3.60E-08	1.70E-06	2.26E-06	2.06E-06	8.12E-07
^{41}Ar	5.06E-13	2.26E-08	2.40E-08	1.34E-08	6.72E-09
^{42}Ar	3.68E-17	7.43E-09	1.07E-08	1.66E-08	2.80E-09
^{43}Ar	9.40E-22	7.18E-12	1.32E-11	8.69E-12	3.15E-12
^{44}Ar	3.77E-26	2.06E-12	2.31E-12	1.27E-12	2.07E-13
^{45}Ar	4.08E-31	1.67E-15	2.05E-15	6.99E-16	2.62E-16
^{46}Ar	6.45E-36	1.84E-16	2.43E-16	1.01E-16	1.15E-17
^{35}K	1.13E-40	1.12E-20	6.53E-21	2.65E-22	4.24E-26
^{36}K	8.84E-35	1.65E-12	5.98E-13	4.78E-15	4.44E-16
^{37}K	1.09E-14	3.49E-08	9.07E-08	6.68E-10	3.34E-10
^{38}K	6.47E-16	1.35E-08	2.38E-08	1.26E-08	1.67E-06
^{39}K	3.61E-06	3.91E-05	4.24E-05	2.01E-04	2.76E-04
^{40}K	1.92E-07	1.20E-06	1.31E-06	1.61E-06	1.21E-06
^{41}K	5.82E-07	3.43E-06	3.76E-06	2.89E-06	2.27E-06
^{42}K	1.15E-10	7.45E-07	9.07E-07	5.61E-07	3.05E-07
^{43}K	6.37E-14	4.80E-07	6.11E-07	2.77E-07	9.30E-08
^{44}K	9.58E-18	9.26E-08	1.33E-07	6.86E-08	1.46E-08
^{45}K	2.39E-21	4.73E-08	8.00E-08	5.25E-08	7.27E-09
^{46}K	6.39E-26	1.98E-09	4.57E-09	4.79E-09	5.43E-10
^{47}K	1.39E-30	8.55E-11	2.39E-10	4.20E-10	3.61E-11
^{48}K	7.22E-36	5.76E-17	2.62E-16	1.78E-16	3.29E-17
^{49}K	7.42E-41	8.97E-19	2.86E-18	2.67E-18	4.49E-19
^{36}Ca	1.48E-50	3.66E-22	6.15E-23	1.25E-24	3.09E-26
^{37}Ca	1.39E-46	1.00E-15	1.27E-16	3.24E-19	8.33E-19
^{38}Ca	5.03E-25	2.29E-10	3.44E-10	2.36E-12	2.88E-09
^{39}Ca	1.40E-25	5.46E-09	8.64E-09	7.46E-10	7.00E-08
^{40}Ca	5.91E-05	5.45E-03	6.89E-03	3.32E-02	3.48E-02

Table 2—Continued

Species	Weak	WS6.8s	WS4.8s	WS1.0s	Strong
^{41}Ca	2.38E-06	8.89E-06	9.26E-06	1.17E-05	9.67E-06
^{42}Ca	5.84E-07	5.83E-05	6.20E-05	4.13E-04	2.14E-04
^{43}Ca	1.13E-07	9.68E-07	1.07E-06	1.29E-06	9.46E-07
^{44}Ca	1.41E-06	8.73E-06	9.85E-06	7.99E-06	6.32E-06
^{45}Ca	1.39E-08	7.69E-07	9.87E-07	8.96E-07	3.68E-07
^{46}Ca	3.09E-09	6.55E-07	9.07E-07	1.55E-06	4.61E-07
^{47}Ca	2.03E-12	4.85E-08	7.88E-08	1.75E-07	2.95E-08
^{48}Ca	1.39E-07	6.44E-07	6.70E-07	5.99E-07	4.81E-07
^{49}Ca	7.30E-13	2.49E-09	2.79E-09	1.89E-09	1.82E-09
^{40}Sc	1.86E-39	8.41E-19	1.21E-18	4.30E-19	5.04E-22
^{41}Sc	9.21E-18	1.29E-11	2.05E-10	1.10E-12	5.09E-15
^{42}Sc	6.68E-18	4.12E-12	1.39E-11	6.62E-11	6.68E-10
^{43}Sc	6.31E-16	1.61E-08	1.20E-07	3.89E-08	1.37E-05
^{44}Sc	1.26E-16	2.66E-09	2.98E-09	2.64E-08	1.94E-08
^{45}Sc	9.38E-08	3.62E-07	3.90E-07	8.97E-07	6.37E-07
^{46}Sc	3.68E-09	2.52E-07	3.17E-07	7.28E-07	3.40E-07
^{47}Sc	3.67E-11	2.65E-07	3.57E-07	8.73E-07	2.65E-07
^{48}Sc	2.74E-14	9.38E-08	1.31E-07	5.35E-07	1.16E-07
^{49}Sc	4.88E-15	3.64E-08	5.45E-08	2.00E-07	3.64E-08
^{50}Sc	5.74E-20	1.01E-10	1.24E-10	2.57E-10	5.30E-11
^{51}Sc	2.04E-24	6.17E-12	9.09E-12	2.05E-11	2.50E-12
^{41}Ti	8.98E-53	7.87E-23	2.30E-23	1.01E-25	2.94E-30
^{42}Ti	7.03E-30	3.52E-15	1.29E-14	1.07E-17	1.07E-15
^{43}Ti	1.19E-27	5.97E-10	1.72E-09	7.14E-11	3.68E-09
^{44}Ti	3.59E-17	2.62E-05	1.99E-04	3.82E-05	1.82E-03
^{45}Ti	7.98E-19	5.00E-08	8.64E-08	2.92E-07	2.28E-07
^{46}Ti	2.24E-07	5.89E-05	6.98E-05	3.12E-04	2.08E-04
^{47}Ti	2.11E-07	1.25E-06	1.18E-06	3.57E-06	2.58E-06
^{48}Ti	2.04E-06	8.25E-06	7.97E-06	1.29E-05	1.14E-05
^{49}Ti	3.26E-07	2.44E-06	2.74E-06	2.55E-06	2.14E-06
^{50}Ti	1.71E-07	2.87E-06	3.47E-06	4.06E-06	2.64E-06

Table 2—Continued

Species	Weak	WS6.8s	WS4.8s	WS1.0s	Strong
^{51}Ti	4.04E-12	8.36E-08	8.35E-08	4.98E-08	2.72E-08
^{52}Ti	2.38E-16	1.32E-08	1.89E-08	2.78E-08	4.26E-09
^{53}Ti	6.20E-21	1.05E-11	2.23E-11	1.02E-11	5.38E-12
^{43}V	3.75E-48	2.47E-27	6.96E-27	7.32E-30	1.14E-33
^{44}V	6.41E-41	2.34E-16	4.54E-16	1.98E-18	7.70E-23
^{45}V	1.06E-28	4.21E-09	1.67E-08	7.50E-11	1.62E-11
^{46}V	1.16E-30	1.12E-10	3.55E-10	7.77E-12	2.02E-09
^{47}V	3.72E-17	5.41E-08	3.28E-07	1.92E-07	1.16E-05
^{48}V	1.20E-16	6.27E-08	5.30E-08	3.32E-07	2.99E-07
^{49}V	2.30E-15	1.15E-07	9.64E-08	1.01E-06	9.04E-07
^{50}V	8.02E-10	1.71E-08	1.97E-08	2.48E-07	2.43E-07
^{51}V	3.79E-07	1.67E-06	1.78E-06	2.37E-06	2.46E-06
^{52}V	9.35E-11	4.95E-07	5.96E-07	5.17E-07	3.07E-07
^{53}V	1.96E-14	2.06E-07	2.72E-07	3.55E-07	8.92E-08
^{54}V	1.34E-18	1.87E-09	2.49E-09	1.43E-09	6.72E-10
^{55}V	6.11E-23	9.31E-11	2.36E-10	4.00E-10	4.88E-11
^{44}Cr	9.37E-63	2.81E-32	2.06E-32	1.62E-37	2.36E-49
^{45}Cr	8.71E-54	2.21E-20	7.97E-21	1.34E-24	9.69E-28
^{46}Cr	4.43E-41	2.92E-12	4.97E-12	1.81E-14	3.97E-12
^{47}Cr	7.52E-40	2.59E-09	1.03E-08	7.56E-10	5.18E-08
^{48}Cr	7.56E-27	2.57E-05	1.14E-04	2.65E-04	1.08E-03
^{49}Cr	1.49E-26	5.08E-07	8.82E-07	4.51E-06	6.25E-06
^{50}Cr	6.46E-07	7.81E-05	1.25E-04	6.99E-04	7.62E-04
^{51}Cr	3.44E-08	1.57E-06	1.58E-06	7.29E-06	5.86E-06
^{52}Cr	1.36E-05	6.70E-05	6.59E-05	1.08E-04	1.08E-04
^{53}Cr	2.22E-06	8.80E-06	8.85E-06	5.93E-06	6.23E-06
^{54}Cr	6.20E-07	1.46E-05	1.82E-05	1.51E-05	8.44E-06
^{55}Cr	2.45E-11	4.71E-07	5.29E-07	2.79E-07	2.03E-07
^{56}Cr	3.40E-15	1.46E-07	1.89E-07	2.42E-07	4.31E-08
^{57}Cr	3.51E-20	9.82E-11	1.73E-10	4.27E-11	3.08E-11
^{58}Cr	4.11E-24	6.63E-12	1.40E-11	1.38E-11	2.52E-12

Table 2—Continued

Species	Weak	WS6.8s	WS4.8s	WS1.0s	Strong
⁴⁶ Mn	7.37E-73	5.21E-33	1.06E-33	1.56E-37	9.42E-47
⁴⁷ Mn	4.38E-58	3.89E-22	4.96E-22	2.16E-24	4.08E-31
⁴⁸ Mn	9.83E-55	3.13E-14	1.50E-14	3.60E-19	2.19E-24
⁴⁹ Mn	1.40E-39	4.72E-09	7.77E-09	3.41E-11	8.93E-11
⁵⁰ Mn	9.57E-40	8.14E-10	4.17E-10	2.19E-10	4.32E-10
⁵¹ Mn	1.61E-17	1.06E-06	2.62E-06	1.21E-05	2.55E-05
⁵² Mn	3.00E-18	8.68E-08	1.14E-07	1.11E-06	1.85E-06
⁵³ Mn	2.09E-15	7.54E-07	8.98E-07	5.76E-06	6.26E-06
⁵⁴ Mn	1.39E-15	7.43E-08	1.17E-07	1.15E-07	1.01E-07
⁵⁵ Mn	1.37E-05	4.73E-05	4.54E-05	3.03E-05	3.22E-05
⁵⁶ Mn	3.17E-09	1.09E-05	1.35E-05	7.12E-06	6.46E-06
⁵⁷ Mn	1.71E-12	8.32E-06	1.04E-05	8.97E-06	2.82E-06
⁵⁸ Mn	1.57E-16	2.34E-07	3.18E-07	1.94E-07	8.00E-08
⁵⁹ Mn	5.32E-20	1.91E-07	3.37E-07	6.50E-07	9.20E-08
⁶⁰ Mn	1.80E-24	1.48E-10	3.69E-10	1.18E-10	5.27E-11
⁶¹ Mn	1.85E-28	1.41E-11	3.56E-11	2.38E-11	4.57E-12
⁴⁷ Fe	1.38E-88	6.03E-39	3.92E-40	2.48E-46	7.33E-64
⁴⁸ Fe	2.69E-73	1.05E-27	3.30E-28	1.23E-32	2.89E-45
⁴⁹ Fe	9.28E-69	2.79E-18	9.59E-20	2.51E-23	3.82E-25
⁵⁰ Fe	3.09E-54	1.84E-13	3.79E-14	3.88E-18	8.09E-18
⁵¹ Fe	1.39E-51	2.85E-11	6.16E-11	1.39E-12	6.95E-11
⁵² Fe	4.50E-28	2.80E-04	6.79E-04	4.98E-03	6.04E-03
⁵³ Fe	7.05E-29	7.45E-06	1.15E-05	7.50E-05	9.13E-05
⁵⁴ Fe	6.24E-05	1.94E-03	3.23E-03	1.95E-02	2.33E-02
⁵⁵ Fe	3.01E-06	3.71E-05	4.49E-05	7.88E-05	8.53E-05
⁵⁶ Fe	1.04E-03	4.15E-03	4.13E-03	3.50E-03	3.25E-03
⁵⁷ Fe	8.50E-05	5.64E-04	6.23E-04	3.72E-04	3.76E-04
⁵⁸ Fe	8.90E-06	7.92E-04	1.04E-03	8.15E-04	4.45E-04
⁵⁹ Fe	6.29E-08	5.49E-05	5.77E-05	3.74E-05	1.68E-05
⁶⁰ Fe	1.83E-09	4.68E-05	6.76E-05	2.89E-04	1.27E-04
⁶¹ Fe	5.93E-14	5.27E-08	1.12E-07	7.32E-08	2.86E-08

Table 2—Continued

Species	Weak	WS6.8s	WS4.8s	WS1.0s	Strong
^{62}Fe	7.30E-18	3.47E-08	4.71E-08	1.52E-07	2.28E-08
^{63}Fe	2.06E-22	5.50E-12	2.26E-11	3.44E-12	2.99E-12
^{50}Co	5.06E-85	1.71E-25	4.72E-27	1.20E-32	6.00E-43
^{51}Co	5.10E-71	1.03E-24	1.57E-25	7.84E-29	3.01E-36
^{52}Co	7.95E-68	2.57E-17	7.36E-18	6.08E-23	1.06E-28
^{53}Co	5.12E-44	8.02E-11	7.40E-11	2.96E-14	5.45E-15
^{54}Co	1.67E-43	5.88E-09	1.71E-09	1.21E-09	6.03E-11
^{55}Co	2.87E-16	1.39E-04	9.78E-05	3.06E-04	3.48E-04
^{56}Co	2.00E-17	6.48E-08	1.36E-07	4.24E-06	2.76E-05
^{57}Co	2.16E-14	8.01E-07	1.05E-06	3.97E-06	3.75E-06
^{58}Co	3.75E-14	3.87E-07	5.97E-07	8.79E-07	8.03E-07
^{59}Co	4.48E-06	5.03E-05	6.79E-05	1.18E-04	1.28E-04
^{60}Co	1.09E-07	7.55E-06	9.15E-06	2.07E-05	9.02E-06
^{61}Co	4.98E-11	2.13E-05	2.84E-05	6.56E-05	3.19E-05
^{62}Co	1.58E-14	1.50E-06	1.67E-06	2.20E-06	6.47E-07
^{63}Co	9.63E-18	3.01E-06	4.70E-06	1.99E-05	3.85E-06
^{64}Co	2.20E-24	1.52E-10	1.12E-10	4.28E-11	4.38E-12
^{65}Co	2.19E-25	5.49E-08	8.58E-08	2.26E-07	2.26E-08
^{51}Ni	4.18E-102	8.40E-33	1.05E-34	1.03E-42	1.90E-61
^{52}Ni	2.70E-88	3.70E-32	1.49E-33	3.68E-39	3.44E-54
^{53}Ni	3.37E-83	1.35E-22	4.71E-24	2.21E-30	3.13E-34
^{54}Ni	3.90E-59	5.40E-16	7.69E-17	7.31E-21	6.07E-20
^{55}Ni	2.29E-56	2.44E-11	2.56E-11	1.23E-13	1.47E-12
^{56}Ni	2.53E-27	1.16E-02	3.56E-02	3.27E-01	9.01E-01
^{57}Ni	2.16E-28	1.59E-04	5.20E-04	2.16E-03	8.61E-03
^{58}Ni	4.41E-05	1.66E-03	3.38E-03	1.25E-02	2.33E-02
^{59}Ni	2.76E-06	3.41E-05	4.69E-05	3.65E-05	7.25E-05
^{60}Ni	1.82E-05	9.61E-05	1.10E-04	5.04E-04	3.96E-04
^{61}Ni	2.17E-06	1.44E-05	1.62E-05	1.67E-05	1.73E-05
^{62}Ni	2.74E-06	3.97E-05	5.09E-05	1.85E-04	1.67E-04
^{63}Ni	1.55E-07	9.35E-06	1.04E-05	8.81E-06	4.43E-06

Table 2—Continued

Species	Weak	WS6.8s	WS4.8s	WS1.0s	Strong
^{64}Ni	7.37E-07	1.67E-05	2.21E-05	4.27E-05	2.25E-05
^{65}Ni	4.55E-11	3.45E-07	4.56E-07	3.37E-07	1.81E-07
^{66}Ni	1.08E-14	2.18E-07	2.95E-07	1.32E-06	5.52E-07
^{67}Ni	4.37E-19	9.24E-10	1.42E-09	7.18E-10	3.18E-10
^{55}Cu	2.76E-88	3.86E-34	1.20E-35	8.93E-43	1.10E-51
^{56}Cu	9.76E-73	3.12E-21	2.82E-21	1.18E-24	1.88E-30
^{57}Cu	1.63E-44	1.08E-11	1.32E-11	3.55E-13	5.04E-16
^{58}Cu	1.20E-40	9.33E-07	1.67E-06	4.67E-07	1.59E-05
^{59}Cu	3.74E-17	5.48E-04	7.25E-04	8.53E-05	7.75E-04
^{60}Cu	2.99E-18	1.96E-05	5.63E-05	3.52E-05	5.51E-04
^{61}Cu	2.27E-17	7.01E-08	3.42E-07	8.57E-07	1.69E-05
^{62}Cu	4.33E-18	6.40E-09	2.76E-08	5.53E-08	6.35E-07
^{63}Cu	5.86E-07	1.59E-06	1.37E-06	1.80E-06	2.18E-06
^{64}Cu	4.70E-10	2.51E-07	3.32E-07	4.54E-07	4.46E-07
^{65}Cu	3.28E-07	1.94E-06	2.29E-06	8.75E-06	9.66E-06
^{66}Cu	1.01E-10	2.64E-07	3.38E-07	4.46E-07	2.71E-07
^{67}Cu	1.64E-13	7.80E-07	9.91E-07	3.25E-06	1.74E-06
^{68}Cu	5.21E-17	4.82E-08	6.80E-08	3.98E-08	2.40E-08
^{69}Cu	3.36E-20	1.36E-07	1.76E-07	4.11E-07	8.07E-08
^{57}Zn	6.78E-89	1.56E-27	2.38E-28	3.92E-34	3.61E-43
^{58}Zn	5.24E-61	1.10E-17	2.67E-18	2.69E-21	7.64E-24
^{59}Zn	3.61E-56	6.11E-11	1.27E-11	2.64E-12	1.38E-11
^{60}Zn	4.53E-29	1.46E-03	3.58E-03	1.83E-03	2.25E-02
^{61}Zn	8.71E-30	3.53E-06	1.45E-05	3.06E-05	4.88E-04
^{62}Zn	1.38E-23	1.17E-04	4.27E-04	6.25E-04	5.91E-03
^{63}Zn	9.44E-25	1.38E-07	3.02E-07	8.68E-08	1.98E-06
^{64}Zn	8.81E-07	2.55E-06	2.30E-06	2.82E-06	3.51E-06
^{65}Zn	4.14E-08	2.89E-07	3.58E-07	3.01E-07	3.96E-07
^{66}Zn	5.65E-07	2.24E-06	2.27E-06	7.47E-06	8.80E-06
^{67}Zn	1.15E-07	4.46E-07	4.55E-07	3.36E-07	3.46E-07
^{68}Zn	3.89E-07	2.62E-06	2.94E-06	2.80E-06	2.63E-06

Table 2—Continued

Species	Weak	WS6.8s	WS4.8s	WS1.0s	Strong
⁶⁹ Zn	4.41E-11	1.81E-07	2.26E-07	1.24E-07	1.10E-07
⁷⁰ Zn	1.28E-08	5.12E-07	6.56E-07	1.16E-06	5.74E-07
⁷¹ Zn	1.27E-12	1.37E-08	2.18E-08	1.05E-08	7.75E-09
⁷² Zn	7.35E-16	2.32E-08	3.02E-08	9.96E-08	3.78E-08
⁵⁹ Ga	1.26E-95	1.16E-38	3.25E-40	4.75E-48	1.90E-62
⁶⁰ Ga	1.28E-80	2.59E-26	1.42E-27	5.11E-30	1.98E-37
⁶¹ Ga	3.12E-46	2.34E-12	4.76E-12	7.89E-15	4.10E-20
⁶² Ga	1.50E-46	6.07E-12	2.00E-12	5.29E-15	1.36E-15
⁶³ Ga	2.77E-35	2.54E-06	4.56E-06	3.41E-07	1.54E-05
⁶⁴ Ga	3.26E-36	7.32E-08	3.79E-07	2.21E-07	1.60E-05
⁶⁵ Ga	4.88E-19	2.43E-09	9.72E-09	1.32E-08	1.01E-06
⁶⁶ Ga	3.80E-20	1.40E-10	9.87E-10	1.50E-09	7.27E-08
⁶⁷ Ga	5.13E-19	4.11E-11	9.43E-11	1.06E-09	2.01E-09
⁶⁸ Ga	1.19E-19	1.73E-11	3.58E-11	3.36E-10	4.44E-10
⁶⁹ Ga	5.69E-08	1.30E-07	1.14E-07	1.39E-07	2.00E-07
⁷⁰ Ga	4.86E-11	1.90E-08	2.39E-08	2.18E-08	2.10E-08
⁷¹ Ga	2.78E-08	1.16E-07	1.18E-07	1.76E-07	1.64E-07
⁷² Ga	3.30E-11	2.94E-08	3.54E-08	2.28E-08	2.27E-08
⁷³ Ga	9.31E-14	7.25E-08	8.78E-08	7.55E-08	5.66E-08
⁷⁴ Ga	6.16E-17	9.96E-09	1.37E-08	6.38E-09	5.58E-09
⁷⁵ Ga	6.58E-20	2.23E-08	2.96E-08	5.27E-08	1.32E-08
⁶² Ge	7.88E-64	3.02E-19	1.19E-19	4.65E-25	1.13E-33
⁶³ Ge	2.39E-59	3.18E-12	1.25E-12	9.95E-14	2.61E-12
⁶⁴ Ge	1.45E-47	2.47E-06	1.09E-05	4.25E-06	3.09E-04
⁶⁵ Ge	3.22E-48	4.09E-08	1.37E-07	1.55E-07	9.67E-06
⁶⁶ Ge	5.78E-31	6.52E-07	3.85E-06	4.91E-06	1.73E-04
⁶⁷ Ge	7.16E-32	3.94E-10	1.81E-09	2.14E-09	1.78E-07
⁶⁸ Ge	1.53E-26	1.03E-11	3.60E-11	9.03E-10	1.04E-08
⁶⁹ Ge	1.00E-27	5.84E-13	1.32E-12	2.88E-11	8.83E-11
⁷⁰ Ge	4.79E-08	1.27E-07	1.14E-07	1.92E-07	2.24E-07
⁷¹ Ge	9.35E-10	1.74E-08	2.17E-08	1.64E-08	1.80E-08

Table 2—Continued

Species	Weak	WS6.8s	WS4.8s	WS1.0s	Strong
⁷² Ge	5.92E-08	2.13E-07	2.09E-07	3.13E-07	3.27E-07
⁷³ Ge	2.05E-08	8.40E-08	8.85E-08	5.77E-08	6.22E-08
⁷⁴ Ge	8.49E-08	3.73E-07	3.86E-07	2.61E-07	2.68E-07
⁷⁵ Ge	2.72E-11	7.66E-08	9.68E-08	5.28E-08	5.15E-08
⁷⁶ Ge	2.97E-14	1.24E-07	1.57E-07	2.03E-07	1.12E-07
⁷⁷ Ge	5.63E-18	3.64E-09	5.73E-09	2.43E-09	1.84E-09
⁷⁸ Ge	2.72E-21	6.67E-09	8.53E-09	1.84E-08	6.41E-09
⁶⁵ As	2.24E-65	5.99E-18	9.62E-18	2.03E-18	5.95E-23
⁶⁶ As	9.96E-66	2.09E-14	4.55E-15	1.83E-18	5.07E-19
⁶⁷ As	9.29E-44	5.07E-10	1.84E-09	1.22E-10	1.44E-08
⁶⁸ As	5.69E-44	1.41E-10	4.34E-10	5.61E-11	2.61E-08
⁶⁹ As	2.39E-38	8.94E-11	4.02E-10	1.30E-11	6.96E-09
⁷⁰ As	2.15E-39	2.91E-12	1.97E-11	1.52E-11	2.62E-09
⁷¹ As	1.48E-20	5.67E-13	1.45E-12	7.92E-13	6.08E-11
⁷² As	4.74E-22	9.22E-14	2.40E-13	1.35E-12	2.26E-12
⁷³ As	2.56E-20	9.36E-12	1.91E-11	2.27E-10	4.23E-10
⁷⁴ As	7.56E-21	3.37E-12	7.67E-12	4.97E-11	7.35E-11
⁷⁵ As	1.11E-14	1.46E-09	2.55E-09	9.08E-09	1.26E-08
⁷⁶ As	8.07E-18	5.02E-11	6.68E-11	3.03E-10	2.41E-10
⁷⁷ As	2.04E-20	1.16E-09	1.67E-09	7.95E-09	7.98E-09
⁷⁸ As	1.71E-23	2.31E-11	2.54E-11	9.98E-11	3.43E-11
⁷⁹ As	3.79E-26	4.97E-10	6.80E-10	3.71E-09	1.73E-09
⁶⁸ Se	1.45E-56	8.60E-10	6.58E-09	1.88E-09	6.63E-07
⁶⁹ Se	2.02E-56	1.32E-09	5.03E-09	7.87E-11	5.68E-08
⁷⁰ Se	1.47E-50	4.03E-09	2.29E-08	1.49E-08	2.02E-06
⁷¹ Se	1.67E-51	1.77E-11	9.61E-11	1.90E-11	5.45E-09
⁷² Se	1.12E-32	4.96E-12	1.08E-11	3.24E-11	2.24E-09
⁷³ Se	3.82E-34	7.50E-15	2.32E-14	4.03E-14	1.35E-12
⁷⁴ Se	4.88E-27	7.52E-11	2.55E-10	5.67E-09	5.67E-09
⁷⁵ Se	3.99E-30	1.08E-12	2.51E-12	5.37E-11	1.01E-10
⁷⁶ Se	2.18E-22	1.81E-10	3.43E-10	1.68E-08	1.42E-08

Table 2—Continued

Species	Weak	WS6.8s	WS4.8s	WS1.0s	Strong
^{77}Se	4.05E-25	1.72E-12	2.67E-12	8.60E-11	1.37E-10
^{78}Se	8.59E-27	4.29E-11	6.73E-11	2.87E-09	3.48E-09
^{79}Se	2.13E-28	2.69E-12	3.49E-12	3.40E-11	1.84E-11
^{80}Se	3.55E-32	5.84E-12	8.54E-12	2.58E-10	2.49E-10
^{81}Se	4.99E-36	2.24E-13	3.21E-13	3.23E-12	1.29E-12
^{82}Se	1.70E-39	5.98E-13	1.30E-12	4.18E-11	3.38E-11
^{83}Se	1.60E-43	3.62E-16	1.75E-15	8.91E-15	3.00E-15
^{70}Br	1.32E-74	1.13E-16	3.21E-17	1.85E-22	3.82E-26
^{71}Br	2.71E-63	2.84E-12	1.02E-11	4.61E-13	1.28E-10
^{72}Br	4.58E-64	8.24E-13	2.96E-12	1.26E-13	3.26E-10
^{73}Br	3.50E-45	1.01E-12	3.59E-12	1.08E-13	1.39E-10
^{74}Br	1.70E-46	1.71E-13	9.16E-13	1.92E-13	1.19E-10
^{75}Br	1.95E-40	9.47E-17	7.89E-16	2.24E-15	9.96E-13
^{76}Br	2.55E-42	5.24E-17	1.35E-16	1.16E-14	4.22E-14
^{77}Br	2.82E-36	5.59E-15	1.13E-14	2.49E-12	3.63E-12
^{78}Br	1.79E-38	8.19E-16	1.51E-15	1.99E-13	6.02E-13
^{79}Br	1.95E-37	1.16E-13	2.02E-13	4.52E-11	7.76E-11
^{80}Br	2.07E-39	1.22E-14	2.05E-14	3.38E-12	9.06E-12
^{81}Br	7.00E-39	1.74E-13	3.17E-13	9.28E-11	1.49E-10
^{82}Br	1.25E-42	5.39E-15	8.02E-15	1.50E-12	2.66E-12
^{83}Br	1.70E-45	7.04E-14	1.23E-13	2.74E-11	4.03E-11
^{72}Kr	1.74E-76	1.52E-12	1.03E-11	7.98E-13	1.67E-09
^{73}Kr	5.61E-77	6.02E-12	3.62E-11	3.66E-13	1.00E-09
^{74}Kr	5.68E-58	6.52E-11	2.95E-10	5.21E-11	2.55E-08
^{75}Kr	3.44E-59	1.74E-14	1.10E-13	1.47E-13	8.50E-11
^{76}Kr	3.11E-53	3.00E-13	8.81E-13	3.81E-13	7.83E-11
^{77}Kr	8.41E-55	5.23E-16	2.70E-15	1.25E-15	3.22E-13
^{78}Kr	2.39E-49	9.15E-15	6.54E-14	4.18E-11	6.65E-11
^{79}Kr	1.36E-51	5.29E-16	1.65E-15	2.06E-12	3.04E-12
^{80}Kr	5.27E-42	3.47E-14	1.18E-13	1.88E-10	2.39E-10
^{81}Kr	1.39E-45	1.15E-16	2.20E-16	4.46E-13	8.27E-13

Table 2—Continued

Species	Weak	WS6.8s	WS4.8s	WS1.0s	Strong
^{82}Kr	4.67E-47	5.17E-15	1.03E-14	4.51E-11	5.76E-11
^{83}Kr	4.63E-49	3.57E-17	6.78E-17	5.71E-14	1.22E-13
^{84}Kr	7.28E-53	3.50E-16	6.01E-16	3.14E-12	4.21E-12
^{85}Kr	1.09E-56	1.73E-18	2.86E-18	2.72E-15	3.23E-15
^{86}Kr	4.35E-60	1.56E-17	3.00E-17	7.31E-14	8.93E-14
^{87}Kr	1.46E-64	3.66E-23	2.05E-22	1.05E-19	9.77E-20

Table 3. Detailed Yields (M_{\odot}) Before Decay of Radioactive Species for $23 M_{\odot}$ Progenitor

Species	Weak	WS6.8s	WS4.8s	WS1.0s	Strong
^3He	2.74E-15	1.10E-13	1.11E-13	9.08E-14	1.11E-14
^4He	4.88E-04	1.23E-03	1.12E-01	1.82E-01	1.55E-01
^6Li	1.92E-21	5.62E-25	1.18E-25	5.87E-26	8.61E-21
^7Li	2.58E-25	1.41E-24	1.58E-24	1.55E-24	3.32E-21
^7Be	5.45E-21	1.96E-18	9.47E-18	7.49E-18	8.79E-19
^8Be	2.92E-11	4.56E-06	7.21E-06	4.85E-06	4.71E-06
^9Be	1.67E-25	2.57E-28	1.55E-27	7.93E-27	1.65E-21
^8B	1.37E-33	3.56E-27	3.30E-24	4.32E-24	4.11E-25
^{10}B	8.88E-22	6.30E-22	3.51E-22	2.91E-22	1.03E-21
^{11}B	3.30E-11	1.14E-13	6.59E-14	3.70E-14	2.63E-13
^{11}C	2.73E-15	2.52E-15	7.46E-16	3.49E-16	1.22E-14
^{12}C	1.98E-01	1.04E-01	1.23E-01	1.18E-01	1.07E-01
^{13}C	8.01E-10	1.48E-10	2.22E-10	2.03E-10	5.31E-10
^{14}C	1.96E-03	1.68E-07	3.13E-08	1.96E-08	3.70E-05
^{12}N	9.30E-31	5.86E-26	2.56E-23	2.60E-23	7.39E-25
^{13}N	2.71E-07	1.45E-08	8.44E-09	7.23E-09	2.17E-08
^{14}N	3.81E-02	2.39E-04	2.83E-04	1.70E-04	5.57E-04
^{15}N	2.31E-02	1.51E-03	8.72E-04	8.14E-04	4.09E-04
^{14}O	2.77E-08	3.11E-05	3.10E-05	2.82E-05	1.19E-06
^{15}O	7.72E-01	7.58E-01	4.95E-01	4.60E-01	3.94E-01
^{16}O	1.06E-01	3.48E-01	1.72E-01	1.64E-01	1.65E-01
^{17}O	1.00E-03	7.10E-06	8.12E-06	4.99E-06	5.50E-06
^{18}O	7.24E-04	1.34E-08	3.58E-09	2.13E-09	1.57E-06
^{19}O	1.64E-11	2.54E-17	2.30E-18	1.42E-18	1.56E-14
^{17}F	1.81E-13	8.23E-11	1.35E-10	1.20E-10	4.22E-11
^{18}F	1.32E-01	1.78E-04	1.01E-04	5.91E-05	8.81E-05
^{19}F	1.39E-02	9.87E-06	8.09E-06	8.05E-06	8.98E-06
^{20}F	1.17E-02	1.65E-12	1.07E-12	8.45E-13	5.57E-04
^{21}F	9.44E-06	7.01E-06	8.77E-06	9.16E-06	8.89E-06
^{17}Ne	2.87E-30	7.72E-18	1.94E-17	1.41E-17	7.70E-18
^{18}Ne	3.42E-10	1.78E-07	1.68E-07	1.18E-07	2.35E-10

Table 3—Continued

Species	Weak	WS6.8s	WS4.8s	WS1.0s	Strong
^{19}Ne	6.97E-02	5.50E-03	4.55E-03	4.37E-03	4.17E-04
^{20}Ne	1.30E-01	1.11E-01	9.70E-02	9.25E-02	8.27E-02
^{21}Ne	5.46E-03	1.18E-06	1.49E-06	1.28E-06	5.97E-05
^{22}Ne	7.91E-02	8.72E-04	1.77E-03	1.22E-03	1.12E-03
^{23}Ne	1.39E-07	3.34E-10	2.21E-10	1.56E-10	1.29E-10
^{24}Ne	2.05E-14	1.20E-17	2.99E-18	2.19E-18	2.58E-18
^{19}Na	1.17E-25	1.97E-18	1.09E-17	9.96E-18	2.53E-19
^{20}Na	3.32E-05	3.08E-05	3.30E-05	3.27E-05	1.07E-08
^{21}Na	3.37E-05	2.81E-05	8.83E-06	7.57E-06	4.61E-07
^{22}Na	7.81E-02	2.93E-03	7.89E-03	6.01E-03	4.02E-03
^{23}Na	4.01E-03	1.12E-03	1.25E-03	1.09E-03	6.85E-04
^{24}Na	1.16E-07	2.67E-09	1.86E-09	1.74E-09	1.82E-09
^{25}Na	3.97E-11	4.82E-12	5.26E-12	4.52E-12	6.70E-12
^{26}Na	8.30E-17	1.14E-17	3.98E-18	3.42E-18	6.30E-18
^{27}Na	1.18E-22	1.05E-23	1.46E-24	1.28E-24	4.16E-24
^{20}Mg	7.15E-30	2.15E-18	5.61E-18	3.30E-18	2.24E-20
^{21}Mg	2.57E-07	1.97E-03	1.49E-03	1.42E-03	5.08E-10
^{22}Mg	1.05E-05	3.17E-03	2.25E-03	2.01E-03	9.66E-05
^{23}Mg	1.44E-02	1.09E-01	9.66E-02	8.93E-02	1.85E-03
^{24}Mg	1.52E-01	3.10E-01	1.27E-01	1.19E-01	1.10E-01
^{25}Mg	5.37E-02	1.57E-02	2.90E-02	2.48E-02	2.16E-02
^{26}Mg	1.68E-03	1.29E-03	9.00E-04	8.00E-04	7.45E-04
^{27}Mg	1.01E-09	3.62E-10	1.86E-10	1.60E-10	1.52E-10
^{28}Mg	1.07E-12	2.92E-13	1.39E-13	1.43E-13	2.13E-13
^{29}Mg	2.27E-19	7.28E-23	1.58E-23	1.60E-23	2.37E-21
^{22}Al	3.96E-26	5.69E-16	1.78E-15	1.84E-15	2.12E-22
^{23}Al	1.65E-18	1.62E-12	3.64E-12	3.61E-12	2.39E-14
^{24}Al	3.12E-05	5.87E-05	7.85E-05	7.65E-05	3.38E-09
^{25}Al	9.35E-04	3.89E-05	1.37E-05	1.16E-05	8.64E-08
^{26}Al	1.38E-03	6.63E-04	6.99E-04	6.38E-04	3.10E-04
^{27}Al	1.08E-02	9.71E-03	7.58E-03	7.13E-03	2.44E-03

Table 3—Continued

Species	Weak	WS6.8s	WS4.8s	WS1.0s	Strong
²⁸ Al	5.93E-04	2.51E-05	3.27E-05	2.95E-05	3.07E-05
²⁹ Al	3.07E-07	1.85E-09	8.42E-10	7.80E-10	1.92E-09
³⁰ Al	9.23E-12	6.05E-15	1.78E-15	1.56E-15	3.45E-14
³¹ Al	1.80E-16	5.73E-20	9.04E-21	7.48E-21	6.82E-19
²³ Si	4.89E-36	5.15E-20	2.24E-19	2.38E-19	4.29E-27
²⁴ Si	2.81E-17	2.10E-10	2.36E-09	1.65E-09	4.24E-12
²⁵ Si	1.25E-05	1.29E-02	1.30E-02	1.24E-02	7.92E-10
²⁶ Si	1.73E-04	1.65E-02	1.30E-02	1.21E-02	1.46E-03
²⁷ Si	1.66E-02	1.89E-01	1.70E-01	1.62E-01	2.02E-02
²⁸ Si	1.23E-01	6.47E-01	3.04E-01	3.23E-01	3.29E-01
²⁹ Si	2.49E-03	4.62E-03	1.92E-03	1.84E-03	1.86E-03
³⁰ Si	5.28E-04	1.30E-03	5.56E-04	6.04E-04	4.73E-04
³¹ Si	1.24E-06	1.11E-07	8.25E-08	7.41E-08	7.31E-08
³² Si	5.41E-10	7.30E-11	1.27E-10	8.44E-11	8.48E-11
³³ Si	6.13E-13	3.94E-18	3.22E-18	2.23E-18	1.42E-13
³⁴ Si	9.78E-17	1.51E-20	5.67E-21	2.42E-21	4.18E-18
²⁷ P	1.19E-12	4.02E-09	9.43E-09	9.05E-09	6.21E-11
²⁸ P	1.74E-05	4.02E-04	5.59E-04	5.38E-04	1.38E-08
²⁹ P	6.91E-06	2.43E-04	1.28E-04	1.02E-04	4.91E-04
³⁰ P	2.59E-03	1.38E-02	1.97E-02	2.62E-02	2.45E-03
³¹ P	1.01E-02	1.36E-02	1.22E-02	1.18E-02	1.68E-03
³² P	6.34E-08	7.50E-08	2.68E-08	2.59E-08	2.69E-08
³³ P	4.56E-08	1.58E-08	3.21E-09	2.85E-09	2.68E-09
³⁴ P	2.82E-04	1.04E-07	7.63E-08	3.13E-08	1.36E-06
³⁵ P	1.06E-07	1.40E-10	1.09E-10	4.84E-11	3.86E-10
³⁶ P	5.59E-13	5.84E-21	2.10E-21	9.66E-22	2.33E-15
³⁷ P	1.41E-17	2.70E-19	4.09E-19	2.06E-19	3.54E-19
³⁸ P	1.95E-24	1.96E-29	1.45E-29	7.46E-30	3.75E-25
²⁸ S	3.17E-19	9.51E-11	3.45E-10	3.96E-10	1.31E-11
²⁹ S	7.60E-09	1.59E-03	2.52E-03	2.23E-03	2.17E-09
³⁰ S	9.48E-08	4.89E-02	8.59E-02	1.01E-01	1.30E-01

Table 3—Continued

Species	Weak	WS6.8s	WS4.8s	WS1.0s	Strong
^{31}S	6.00E-03	9.98E-02	9.42E-02	9.03E-02	9.32E-02
^{32}S	1.81E-02	2.57E-01	2.06E-01	2.42E-01	2.51E-01
^{33}S	1.59E-03	4.16E-03	1.48E-03	1.31E-03	1.33E-03
^{34}S	8.09E-04	5.39E-04	5.63E-04	6.16E-04	1.31E-04
^{35}S	5.42E-07	3.80E-08	8.72E-08	6.18E-08	6.17E-08
^{36}S	2.52E-06	2.58E-07	1.38E-07	1.16E-07	1.11E-07
^{37}S	2.87E-06	2.20E-15	7.92E-16	7.12E-16	1.69E-08
^{38}S	4.37E-10	3.69E-12	7.76E-12	4.69E-12	5.80E-12
^{39}S	9.35E-15	1.14E-19	1.01E-19	6.29E-20	5.66E-17
^{40}S	6.60E-19	9.68E-20	2.75E-19	1.95E-19	1.99E-19
^{41}S	1.41E-24	4.75E-29	7.87E-29	5.63E-29	5.29E-26
^{42}S	2.93E-29	2.41E-29	8.09E-29	5.63E-29	6.75E-29
^{31}Cl	1.51E-19	7.81E-12	4.83E-10	1.36E-10	3.21E-10
^{32}Cl	1.71E-10	3.70E-07	4.94E-06	9.83E-07	4.45E-07
^{33}Cl	3.30E-07	1.24E-07	4.02E-07	1.04E-07	4.08E-05
^{34}Cl	7.72E-04	8.52E-03	1.40E-02	1.66E-02	2.64E-03
^{35}Cl	1.52E-03	4.15E-03	6.36E-03	6.25E-03	7.35E-04
^{36}Cl	7.04E-06	2.77E-08	1.95E-08	1.34E-08	4.86E-08
^{37}Cl	1.71E-06	5.11E-07	7.47E-07	5.99E-07	5.69E-07
^{38}Cl	7.87E-05	3.81E-07	1.03E-06	6.46E-07	9.13E-07
^{39}Cl	8.59E-08	2.34E-09	5.39E-09	3.87E-09	4.00E-09
^{40}Cl	1.35E-11	1.19E-12	3.21E-12	2.34E-12	2.44E-12
^{41}Cl	5.40E-15	2.31E-15	5.21E-15	4.43E-15	4.54E-15
^{42}Cl	5.41E-19	4.44E-19	1.33E-18	9.83E-19	1.20E-18
^{43}Cl	6.36E-23	2.56E-22	6.12E-22	5.83E-22	6.28E-22
^{44}Cl	2.32E-28	5.53E-31	1.09E-30	1.04E-30	3.48E-29
^{45}Cl	1.90E-32	2.25E-31	7.10E-31	6.03E-31	7.44E-31
^{32}Ar	1.39E-24	7.27E-13	3.35E-10	1.06E-10	2.99E-11
^{33}Ar	1.07E-13	1.10E-05	4.41E-04	3.87E-05	7.55E-06
^{34}Ar	1.54E-08	1.40E-02	4.49E-02	4.56E-02	6.52E-02
^{35}Ar	5.12E-04	2.12E-02	3.70E-02	3.35E-02	3.63E-02

Table 3—Continued

Species	Weak	WS6.8s	WS4.8s	WS1.0s	Strong
^{36}Ar	8.25E-04	5.93E-02	7.84E-02	9.02E-02	9.16E-02
^{37}Ar	2.18E-04	7.23E-04	2.96E-04	2.43E-04	2.65E-04
^{38}Ar	3.38E-05	2.70E-05	3.79E-05	3.71E-05	2.33E-05
^{39}Ar	9.78E-08	1.54E-08	3.46E-08	2.82E-08	2.76E-08
^{40}Ar	7.20E-08	7.31E-08	6.58E-08	5.56E-08	4.85E-08
^{41}Ar	4.73E-06	6.48E-08	2.05E-07	1.48E-07	1.57E-07
^{42}Ar	3.17E-09	8.63E-10	1.37E-09	1.27E-09	1.22E-09
^{43}Ar	3.57E-13	6.75E-14	1.67E-13	1.23E-13	1.45E-13
^{44}Ar	6.07E-17	7.41E-17	1.53E-16	1.48E-16	1.54E-16
^{45}Ar	2.81E-21	5.41E-21	1.49E-20	1.18E-20	1.56E-20
^{46}Ar	2.01E-25	3.15E-24	6.49E-24	7.05E-24	8.05E-24
^{35}K	1.36E-21	3.02E-14	1.41E-10	4.07E-11	1.08E-10
^{36}K	5.25E-12	2.49E-09	6.60E-06	8.29E-07	8.21E-07
^{37}K	4.55E-09	7.36E-09	9.67E-07	3.85E-08	1.40E-06
^{38}K	3.81E-05	3.21E-04	7.87E-04	7.18E-04	1.89E-04
^{39}K	2.28E-04	9.79E-04	1.92E-03	1.84E-03	4.63E-04
^{40}K	8.89E-07	7.32E-08	1.34E-07	1.14E-07	1.10E-07
^{41}K	7.82E-07	3.05E-07	6.04E-07	5.26E-07	4.92E-07
^{42}K	7.21E-05	2.50E-06	6.31E-06	4.97E-06	4.94E-06
^{43}K	3.32E-07	4.20E-08	8.65E-08	7.44E-08	7.31E-08
^{44}K	2.50E-10	1.31E-10	2.30E-10	2.16E-10	2.16E-10
^{45}K	2.35E-13	3.93E-13	6.51E-13	6.52E-13	6.68E-13
^{46}K	2.67E-17	1.59E-16	2.57E-16	2.75E-16	2.91E-16
^{47}K	2.21E-21	3.86E-20	6.40E-20	7.26E-20	8.02E-20
^{48}K	5.08E-26	1.86E-27	2.88E-27	3.29E-27	1.17E-26
^{49}K	2.93E-30	2.44E-28	5.47E-28	6.11E-28	7.94E-28
^{36}Ca	4.73E-21	6.25E-15	7.63E-09	2.50E-09	1.03E-10
^{37}Ca	1.51E-14	5.54E-08	1.34E-03	8.91E-05	6.22E-06
^{38}Ca	1.70E-10	1.68E-04	3.35E-03	1.39E-03	2.51E-03
^{39}Ca	1.50E-05	1.72E-03	5.91E-03	4.14E-03	5.30E-03
^{40}Ca	9.00E-05	5.37E-02	9.97E-02	1.06E-01	1.07E-01

Table 3—Continued

Species	Weak	WS6.8s	WS4.8s	WS1.0s	Strong
^{41}Ca	4.31E-06	2.00E-05	1.66E-05	1.72E-05	1.74E-05
^{42}Ca	2.49E-05	3.06E-05	3.30E-05	4.68E-05	2.75E-05
^{43}Ca	2.10E-06	4.84E-07	5.90E-07	5.53E-07	4.87E-07
^{44}Ca	6.05E-08	3.18E-08	3.89E-08	4.38E-08	3.43E-08
^{45}Ca	5.48E-08	4.70E-09	8.98E-09	7.68E-09	7.30E-09
^{46}Ca	3.36E-10	2.03E-10	2.09E-10	1.98E-10	1.84E-10
^{47}Ca	4.98E-08	3.60E-09	7.37E-09	6.21E-09	5.94E-09
^{48}Ca	6.94E-11	7.07E-12	8.22E-12	8.00E-12	7.37E-12
^{49}Ca	3.97E-14	1.95E-17	8.33E-17	3.59E-17	3.07E-16
^{40}Sc	1.50E-19	2.72E-13	4.23E-09	2.13E-09	6.97E-10
^{41}Sc	9.35E-15	4.63E-11	5.18E-07	8.46E-08	9.90E-08
^{42}Sc	4.22E-10	5.25E-08	5.76E-07	1.97E-07	8.88E-08
^{43}Sc	5.55E-07	2.20E-06	4.17E-06	6.63E-06	1.48E-06
^{44}Sc	2.15E-07	1.10E-07	1.22E-07	1.19E-07	9.33E-08
^{45}Sc	6.92E-08	4.92E-08	2.73E-07	5.13E-07	1.81E-07
^{46}Sc	1.75E-09	1.18E-09	1.35E-09	1.39E-09	1.21E-09
^{47}Sc	4.92E-09	4.19E-09	5.04E-09	4.82E-09	4.10E-09
^{48}Sc	1.80E-11	1.34E-11	1.19E-11	1.18E-11	1.00E-11
^{49}Sc	5.55E-12	3.93E-13	2.94E-13	3.04E-13	2.29E-13
^{50}Sc	1.98E-16	1.64E-17	1.67E-17	1.86E-17	1.63E-17
^{51}Sc	2.07E-20	2.26E-21	1.82E-21	2.29E-21	2.34E-21
^{41}Ti	1.66E-22	6.37E-14	2.59E-07	1.42E-07	1.36E-09
^{42}Ti	2.59E-16	1.97E-08	1.18E-03	2.97E-04	1.75E-04
^{43}Ti	1.08E-11	5.26E-07	8.25E-04	2.06E-04	8.66E-05
^{44}Ti	1.46E-06	7.56E-05	1.66E-04	1.95E-04	1.36E-04
^{45}Ti	3.98E-07	5.19E-07	3.57E-07	3.44E-07	2.76E-07
^{46}Ti	3.93E-07	1.02E-06	2.45E-05	4.25E-05	1.60E-05
^{47}Ti	2.97E-06	6.03E-07	7.24E-07	6.77E-07	5.77E-07
^{48}Ti	8.94E-07	2.55E-07	3.67E-07	4.64E-07	2.69E-07
^{49}Ti	3.67E-07	6.72E-08	9.42E-08	8.58E-08	7.52E-08
^{50}Ti	1.50E-09	1.64E-07	1.23E-09	1.25E-09	1.13E-09

Table 3—Continued

Species	Weak	WS6.8s	WS4.8s	WS1.0s	Strong
^{51}Ti	5.78E-13	9.85E-13	7.38E-13	7.75E-13	7.62E-13
^{52}Ti	5.61E-16	7.62E-15	4.43E-16	5.02E-16	5.20E-16
^{53}Ti	4.49E-21	9.97E-21	3.32E-20	2.26E-20	5.35E-20
^{43}V	2.72E-29	7.08E-18	1.24E-10	5.40E-11	4.60E-11
^{44}V	5.82E-19	3.33E-13	2.02E-07	5.29E-08	1.33E-08
^{45}V	6.48E-13	7.12E-10	3.16E-07	5.81E-08	5.22E-09
^{46}V	2.52E-10	1.60E-07	1.15E-06	1.08E-06	2.83E-07
^{47}V	2.20E-08	3.46E-07	1.11E-05	1.94E-05	5.10E-06
^{48}V	1.50E-07	2.80E-07	3.25E-07	4.75E-07	2.00E-07
^{49}V	3.56E-07	2.59E-07	1.32E-06	2.39E-06	8.95E-07
^{50}V	6.99E-07	1.45E-07	1.81E-07	1.67E-07	1.39E-07
^{51}V	9.79E-08	1.29E-07	6.83E-08	6.86E-08	6.15E-08
^{52}V	2.47E-10	5.40E-10	4.80E-10	5.09E-10	4.96E-10
^{53}V	1.35E-13	4.80E-12	7.07E-13	7.97E-13	8.16E-13
^{54}V	1.96E-17	2.14E-16	3.42E-16	3.96E-16	4.51E-16
^{55}V	5.63E-21	2.56E-19	4.05E-19	5.13E-19	6.78E-19
^{44}Cr	1.63E-34	8.89E-18	1.74E-08	9.66E-09	4.37E-10
^{45}Cr	4.82E-22	1.02E-11	2.42E-04	8.79E-05	1.31E-06
^{46}Cr	1.04E-15	2.96E-07	3.24E-04	2.27E-04	3.18E-04
^{47}Cr	3.55E-12	6.26E-07	3.93E-06	3.50E-06	1.85E-05
^{48}Cr	4.13E-07	2.22E-04	5.92E-04	5.19E-04	5.07E-04
^{49}Cr	1.02E-06	2.22E-06	1.43E-06	1.77E-06	1.16E-06
^{50}Cr	4.05E-07	1.13E-05	2.86E-05	4.09E-05	1.86E-05
^{51}Cr	2.24E-05	5.98E-06	6.32E-06	5.93E-06	4.83E-06
^{52}Cr	4.05E-06	1.97E-04	1.80E-06	2.29E-06	1.32E-06
^{53}Cr	1.97E-06	1.93E-06	6.66E-07	6.28E-07	4.96E-07
^{54}Cr	7.89E-08	1.82E-05	5.22E-08	5.15E-08	4.71E-08
^{55}Cr	2.73E-11	5.32E-11	5.06E-11	5.14E-11	4.98E-11
^{56}Cr	1.25E-14	3.33E-12	6.33E-14	7.05E-14	7.19E-14
^{57}Cr	5.75E-19	1.06E-19	1.68E-19	1.58E-19	1.81E-18
^{58}Cr	1.49E-22	7.22E-21	1.23E-20	1.54E-20	1.82E-20

Table 3—Continued

Species	Weak	WS6.8s	WS4.8s	WS1.0s	Strong
⁴⁶ Mn	1.78E-35	3.98E-21	1.96E-11	1.36E-11	2.39E-13
⁴⁷ Mn	2.08E-26	1.80E-15	1.22E-09	1.00E-09	9.43E-10
⁴⁸ Mn	1.78E-18	4.62E-08	5.31E-06	9.21E-06	4.90E-05
⁴⁹ Mn	6.44E-16	1.22E-09	2.02E-07	1.55E-07	9.60E-08
⁵⁰ Mn	3.11E-10	1.74E-07	3.77E-06	1.88E-06	1.75E-07
⁵¹ Mn	6.30E-08	1.60E-06	2.26E-05	1.94E-05	4.43E-06
⁵² Mn	9.58E-07	2.26E-06	1.65E-06	1.90E-06	9.90E-07
⁵³ Mn	4.07E-05	2.05E-05	1.89E-05	1.84E-05	1.57E-05
⁵⁴ Mn	2.25E-05	2.67E-06	4.40E-06	3.84E-06	3.42E-06
⁵⁵ Mn	5.01E-07	1.04E-05	3.93E-07	3.94E-07	3.64E-07
⁵⁶ Mn	1.11E-09	8.06E-09	2.29E-09	2.48E-09	2.43E-09
⁵⁷ Mn	1.45E-12	6.62E-10	7.22E-12	8.25E-12	8.47E-12
⁵⁸ Mn	3.60E-16	7.43E-15	7.18E-15	8.68E-15	9.77E-15
⁵⁹ Mn	3.83E-19	2.44E-17	1.94E-17	2.50E-17	2.87E-17
⁶⁰ Mn	4.69E-23	9.71E-23	2.81E-22	2.21E-22	1.67E-21
⁶¹ Mn	2.40E-26	7.74E-24	1.40E-23	1.97E-23	2.81E-23
⁴⁷ Fe	4.90E-42	5.54E-25	8.37E-13	7.14E-13	1.57E-15
⁴⁸ Fe	2.09E-32	4.73E-15	1.14E-07	1.96E-07	6.00E-08
⁴⁹ Fe	1.71E-21	1.83E-09	6.67E-05	4.92E-05	2.94E-05
⁵⁰ Fe	2.00E-20	4.74E-08	1.26E-04	1.56E-04	2.86E-04
⁵¹ Fe	2.42E-14	9.88E-07	1.22E-04	3.25E-04	4.62E-04
⁵² Fe	1.12E-06	3.86E-03	1.31E-02	8.21E-03	8.94E-03
⁵³ Fe	6.57E-05	6.38E-05	3.25E-05	3.03E-05	2.51E-05
⁵⁴ Fe	2.12E-05	6.87E-03	6.33E-05	6.78E-05	4.18E-05
⁵⁵ Fe	1.78E-03	6.34E-04	5.57E-04	5.19E-04	4.22E-04
⁵⁶ Fe	2.44E-04	1.61E-02	2.46E-04	1.30E-04	1.68E-04
⁵⁷ Fe	5.10E-05	1.05E-04	2.14E-05	2.01E-05	1.50E-05
⁵⁸ Fe	1.46E-06	8.42E-04	3.16E-06	1.79E-06	1.73E-06
⁵⁹ Fe	5.29E-08	5.07E-08	5.01E-08	4.88E-08	3.24E-08
⁶⁰ Fe	3.72E-10	8.89E-09	3.58E-10	3.65E-10	2.85E-10
⁶¹ Fe	2.53E-13	6.45E-14	1.56E-13	1.08E-13	1.70E-13

Table 3—Continued

Species	Weak	WS6.8s	WS4.8s	WS1.0s	Strong
^{62}Fe	6.27E-14	4.92E-16	6.29E-16	7.12E-16	7.22E-16
^{63}Fe	7.08E-21	6.67E-23	9.56E-23	1.07E-22	1.50E-21
^{50}Co	1.57E-29	9.39E-16	1.03E-08	7.46E-09	1.66E-09
^{51}Co	1.69E-32	2.50E-17	6.81E-11	7.86E-11	1.58E-10
^{52}Co	2.37E-21	3.25E-11	1.73E-06	3.32E-06	1.85E-06
^{53}Co	2.83E-19	3.16E-11	8.51E-06	3.22E-06	1.19E-06
^{54}Co	3.46E-09	2.68E-06	1.30E-05	3.83E-06	1.88E-06
^{55}Co	1.01E-06	1.19E-04	5.28E-05	1.94E-05	5.08E-06
^{56}Co	5.17E-05	1.44E-04	6.92E-05	6.61E-05	5.13E-05
^{57}Co	2.47E-05	8.74E-05	1.97E-05	1.83E-05	1.54E-05
^{58}Co	1.96E-05	8.18E-06	6.37E-06	5.90E-06	4.30E-06
^{59}Co	9.20E-07	4.55E-05	3.13E-06	1.84E-06	1.96E-06
^{60}Co	1.45E-08	6.82E-08	1.50E-08	1.41E-08	9.00E-09
^{61}Co	1.29E-10	6.98E-08	7.78E-10	6.43E-10	4.87E-10
^{62}Co	1.61E-13	2.46E-12	7.67E-13	8.48E-13	7.45E-13
^{63}Co	6.36E-16	1.04E-13	6.02E-15	7.03E-15	6.73E-15
^{64}Co	2.10E-20	1.94E-18	3.10E-18	3.93E-18	1.05E-17
^{65}Co	3.18E-22	2.93E-20	4.03E-20	5.28E-20	5.96E-20
^{51}Ni	1.32E-37	7.51E-22	2.52E-12	2.23E-12	1.43E-13
^{52}Ni	1.81E-40	1.48E-19	9.19E-11	1.27E-10	3.56E-11
^{53}Ni	5.38E-26	8.21E-12	1.17E-04	1.02E-04	5.32E-06
^{54}Ni	2.64E-24	3.48E-09	6.13E-04	4.06E-04	5.09E-04
^{55}Ni	3.53E-14	1.13E-05	1.67E-03	7.56E-04	5.34E-04
^{56}Ni	7.55E-05	8.22E-02	7.68E-01	6.80E-01	6.40E-01
^{57}Ni	2.77E-04	1.46E-03	8.37E-04	7.45E-04	6.89E-04
^{58}Ni	1.38E-04	2.86E-02	2.07E-02	1.68E-02	2.18E-02
^{59}Ni	3.98E-05	3.12E-04	2.12E-04	1.89E-04	2.06E-04
^{60}Ni	8.26E-06	2.99E-02	3.45E-02	2.98E-02	3.34E-02
^{61}Ni	6.33E-06	6.49E-05	9.10E-05	9.09E-05	7.66E-05
^{62}Ni	7.91E-07	5.35E-03	8.72E-03	8.70E-03	5.28E-03
^{63}Ni	1.84E-06	9.00E-07	1.03E-06	1.18E-06	6.59E-07

Table 3—Continued

Species	Weak	WS6.8s	WS4.8s	WS1.0s	Strong
^{64}Ni	1.94E-08	3.57E-06	1.95E-06	2.53E-06	8.21E-07
^{65}Ni	9.72E-12	1.18E-11	1.76E-11	1.77E-11	1.52E-11
^{66}Ni	1.97E-14	1.27E-11	2.15E-12	3.55E-12	6.41E-13
^{67}Ni	1.23E-18	1.20E-17	2.01E-17	2.08E-17	2.41E-17
^{55}Cu	3.04E-43	1.32E-23	1.91E-14	2.63E-14	1.28E-13
^{56}Cu	6.18E-25	9.13E-14	4.58E-09	2.83E-09	1.68E-09
^{57}Cu	2.43E-22	1.18E-12	2.36E-05	2.40E-05	9.28E-06
^{58}Cu	1.77E-10	7.53E-05	7.31E-05	6.96E-05	3.57E-05
^{59}Cu	1.94E-10	4.96E-05	6.41E-05	6.24E-05	3.28E-05
^{60}Cu	2.88E-08	8.33E-07	2.60E-06	3.30E-06	1.58E-06
^{61}Cu	2.81E-08	4.33E-06	1.14E-04	1.81E-04	9.69E-05
^{62}Cu	1.32E-06	1.02E-06	6.26E-06	8.38E-06	5.39E-06
^{63}Cu	4.53E-07	7.66E-06	1.69E-04	2.05E-04	1.24E-04
^{64}Cu	7.71E-07	2.22E-07	1.56E-06	2.12E-06	1.06E-06
^{65}Cu	2.59E-08	3.61E-07	5.06E-06	7.63E-06	2.65E-06
^{66}Cu	8.19E-11	1.91E-10	7.55E-10	1.41E-09	4.58E-10
^{67}Cu	1.07E-12	4.97E-11	2.45E-10	5.55E-10	1.06E-10
^{68}Cu	6.94E-16	7.06E-15	1.02E-14	1.27E-14	1.14E-14
^{69}Cu	5.23E-17	1.72E-16	1.28E-16	1.70E-16	1.46E-16
^{57}Zn	8.69E-31	3.40E-18	7.70E-11	4.56E-11	3.95E-12
^{58}Zn	1.35E-27	1.82E-14	1.91E-04	2.01E-04	4.31E-06
^{59}Zn	3.20E-15	8.39E-05	3.35E-04	3.76E-04	3.35E-04
^{60}Zn	3.04E-09	1.05E-04	5.63E-03	6.90E-03	5.36E-03
^{61}Zn	2.89E-08	2.75E-06	1.35E-05	1.32E-05	9.45E-06
^{62}Zn	1.60E-06	5.94E-05	2.38E-03	1.90E-03	1.97E-03
^{63}Zn	1.59E-06	2.53E-06	3.89E-05	4.02E-05	2.92E-05
^{64}Zn	1.17E-06	3.16E-04	9.30E-03	9.49E-03	7.51E-03
^{65}Zn	1.06E-06	7.12E-07	2.24E-05	3.17E-05	1.61E-05
^{66}Zn	3.31E-07	3.84E-05	4.58E-03	8.04E-03	2.94E-03
^{67}Zn	7.02E-07	1.58E-07	4.99E-07	9.47E-07	3.22E-07
^{68}Zn	1.93E-08	1.74E-07	1.57E-05	4.06E-05	7.24E-06

Table 3—Continued

Species	Weak	WS6.8s	WS4.8s	WS1.0s	Strong
⁶⁹ Zn	1.77E-08	2.14E-09	3.88E-09	3.62E-09	2.34E-09
⁷⁰ Zn	2.45E-08	2.87E-08	2.37E-08	2.41E-08	2.22E-08
⁷¹ Zn	7.74E-08	7.81E-09	1.19E-08	9.90E-09	5.07E-09
⁷² Zn	4.79E-10	3.16E-10	3.48E-10	3.45E-10	3.14E-10
⁵⁹ Ga	1.68E-49	4.13E-29	1.86E-16	5.01E-16	6.35E-17
⁶⁰ Ga	1.56E-31	4.69E-16	6.30E-13	1.11E-12	2.84E-12
⁶¹ Ga	3.04E-24	1.68E-12	9.64E-08	1.13E-07	4.55E-08
⁶² Ga	3.17E-19	5.30E-07	6.12E-07	6.05E-07	8.73E-08
⁶³ Ga	2.37E-17	1.83E-06	1.56E-06	1.45E-06	1.54E-07
⁶⁴ Ga	1.86E-10	1.74E-07	5.43E-07	7.35E-07	2.94E-07
⁶⁵ Ga	9.00E-12	4.05E-08	1.95E-06	3.96E-06	1.35E-06
⁶⁶ Ga	2.60E-08	6.90E-08	7.35E-07	1.22E-06	4.80E-07
⁶⁷ Ga	2.11E-08	5.52E-08	6.02E-06	1.45E-05	4.25E-06
⁶⁸ Ga	3.94E-09	1.08E-08	1.25E-07	2.73E-07	8.08E-08
⁶⁹ Ga	4.75E-09	7.75E-09	2.41E-06	6.81E-06	1.32E-06
⁷⁰ Ga	5.10E-08	1.28E-08	1.57E-08	2.16E-08	1.14E-08
⁷¹ Ga	1.96E-08	2.20E-08	1.76E-08	2.36E-08	1.48E-08
⁷² Ga	8.09E-08	1.20E-08	1.95E-08	1.74E-08	1.01E-08
⁷³ Ga	2.47E-09	1.54E-09	1.75E-09	1.73E-09	1.53E-09
⁷⁴ Ga	6.64E-12	7.30E-12	1.22E-11	1.23E-11	1.14E-11
⁷⁵ Ga	3.19E-14	1.32E-13	1.72E-13	1.92E-13	1.92E-13
⁶² Ge	3.72E-31	9.77E-14	1.49E-06	2.18E-06	5.91E-08
⁶³ Ge	8.19E-23	3.40E-06	1.38E-05	1.63E-05	5.11E-06
⁶⁴ Ge	1.19E-12	2.54E-06	4.49E-05	5.16E-05	2.77E-05
⁶⁵ Ge	1.35E-12	4.99E-07	6.44E-07	8.09E-07	1.77E-07
⁶⁶ Ge	3.45E-08	1.52E-06	3.23E-05	2.56E-05	2.09E-05
⁶⁷ Ge	6.30E-08	1.93E-07	1.34E-06	1.68E-06	7.89E-07
⁶⁸ Ge	1.52E-07	9.85E-07	3.97E-04	4.14E-04	2.58E-04
⁶⁹ Ge	9.24E-10	3.88E-09	1.31E-06	2.28E-06	7.56E-07
⁷⁰ Ge	4.36E-08	1.67E-07	3.97E-04	1.09E-03	2.67E-04
⁷¹ Ge	1.07E-07	4.38E-08	4.84E-07	1.77E-06	3.14E-07

Table 3—Continued

Species	Weak	WS6.8s	WS4.8s	WS1.0s	Strong
⁷² Ge	5.77E-08	5.67E-08	1.95E-05	1.03E-04	1.14E-05
⁷³ Ge	1.57E-07	2.61E-08	4.22E-08	4.18E-08	2.60E-08
⁷⁴ Ge	3.15E-09	2.10E-09	2.92E-08	1.98E-07	1.20E-08
⁷⁵ Ge	1.00E-11	1.46E-11	2.11E-11	2.55E-11	2.04E-11
⁷⁶ Ge	3.73E-14	1.62E-13	1.07E-12	9.29E-12	4.43E-13
⁷⁷ Ge	1.88E-17	2.08E-16	3.55E-16	3.87E-16	4.23E-16
⁷⁸ Ge	2.96E-20	1.13E-18	1.86E-18	4.80E-18	2.38E-18
⁶⁵ As	1.55E-34	1.16E-15	1.82E-11	2.43E-11	1.32E-11
⁶⁶ As	4.66E-22	2.78E-07	4.70E-07	4.77E-07	4.00E-08
⁶⁷ As	1.39E-20	1.91E-08	2.91E-08	2.86E-08	6.33E-10
⁶⁸ As	9.04E-17	1.38E-08	8.58E-09	7.90E-09	1.23E-10
⁶⁹ As	8.40E-16	1.09E-08	1.41E-08	2.12E-08	3.99E-09
⁷⁰ As	2.60E-11	1.42E-09	1.44E-08	3.05E-08	5.91E-09
⁷¹ As	1.46E-10	1.47E-09	7.29E-08	3.04E-07	4.67E-08
⁷² As	1.53E-09	4.39E-09	3.41E-09	8.23E-09	2.13E-09
⁷³ As	7.93E-09	1.87E-08	1.52E-07	8.28E-07	1.02E-07
⁷⁴ As	1.35E-10	7.88E-10	1.54E-09	8.61E-09	7.95E-10
⁷⁵ As	1.32E-10	2.86E-10	1.78E-08	1.37E-07	8.47E-09
⁷⁶ As	2.34E-13	9.37E-13	1.03E-11	1.13E-10	4.78E-12
⁷⁷ As	1.52E-15	1.02E-14	1.23E-11	1.36E-10	3.91E-12
⁷⁸ As	3.75E-19	1.48E-17	2.22E-16	3.45E-15	7.75E-17
⁷⁹ As	2.45E-21	2.03E-19	1.81E-16	3.13E-15	4.64E-17
⁶⁸ Se	9.81E-16	9.07E-08	4.40E-07	4.59E-07	1.25E-07
⁶⁹ Se	4.87E-15	1.96E-07	1.95E-07	1.82E-07	5.29E-10
⁷⁰ Se	3.98E-10	1.57E-07	3.12E-07	2.59E-07	8.39E-08
⁷¹ Se	3.98E-10	4.09E-09	2.50E-08	3.31E-08	1.04E-08
⁷² Se	5.95E-08	1.68E-07	6.81E-06	7.62E-06	3.93E-06
⁷³ Se	1.27E-09	3.99E-09	4.55E-08	8.57E-08	2.40E-08
⁷⁴ Se	2.53E-08	5.45E-08	1.39E-05	5.96E-05	1.22E-05
⁷⁵ Se	5.72E-11	1.43E-10	1.11E-07	7.01E-07	9.20E-08
⁷⁶ Se	2.20E-11	1.04E-10	8.03E-06	6.80E-05	6.00E-06

Table 3—Continued

Species	Weak	WS6.8s	WS4.8s	WS1.0s	Strong
^{77}Se	4.39E-15	1.20E-13	1.28E-08	1.50E-07	9.21E-09
^{78}Se	2.24E-17	3.42E-12	2.96E-07	3.50E-06	1.32E-07
^{79}Se	8.61E-22	2.54E-16	1.47E-11	2.55E-10	6.34E-12
^{80}Se	7.17E-24	8.39E-15	3.66E-10	5.90E-09	1.01E-10
^{81}Se	5.70E-28	4.69E-19	1.13E-14	2.56E-13	3.12E-15
^{82}Se	5.62E-30	7.46E-19	1.26E-14	3.04E-13	2.64E-15
^{83}Se	1.61E-36	3.80E-26	4.07E-22	2.03E-20	8.04E-23
^{70}Br	3.21E-30	4.29E-12	2.75E-11	2.33E-11	4.97E-13
^{71}Br	8.24E-25	1.60E-09	2.47E-09	2.42E-09	7.42E-12
^{72}Br	4.01E-20	1.12E-09	8.71E-10	7.98E-10	1.61E-13
^{73}Br	1.12E-17	2.76E-09	2.02E-09	1.89E-09	1.72E-11
^{74}Br	2.47E-11	7.25E-10	9.16E-10	1.49E-09	2.39E-10
^{75}Br	1.86E-11	3.68E-09	4.70E-09	1.38E-08	1.76E-09
^{76}Br	2.22E-11	6.63E-11	9.13E-10	5.04E-09	7.39E-10
^{77}Br	8.88E-12	2.07E-11	1.90E-08	1.72E-07	1.54E-08
^{78}Br	2.47E-15	6.37E-15	4.98E-10	5.65E-09	3.98E-10
^{79}Br	6.96E-18	1.59E-14	2.87E-08	3.57E-07	1.51E-08
^{80}Br	6.47E-21	2.04E-16	3.42E-10	5.63E-09	1.67E-10
^{81}Br	2.31E-23	1.41E-15	1.48E-09	2.56E-08	5.22E-10
^{82}Br	1.30E-26	1.97E-18	1.45E-12	3.47E-11	4.73E-13
^{83}Br	6.44E-29	7.46E-18	3.32E-12	8.05E-11	7.89E-13
^{72}Kr	3.28E-19	7.01E-09	1.07E-08	9.23E-09	7.79E-10
^{73}Kr	4.03E-17	1.65E-08	1.67E-08	1.55E-08	8.09E-12
^{74}Kr	9.36E-12	3.89E-08	3.71E-08	3.55E-08	9.88E-10
^{75}Kr	1.05E-10	1.57E-09	1.32E-09	1.42E-09	4.39E-10
^{76}Kr	2.17E-08	1.10E-07	1.09E-07	1.44E-07	8.85E-08
^{77}Kr	1.29E-10	3.93E-10	4.35E-09	9.89E-09	3.32E-09
^{78}Kr	7.42E-11	1.77E-10	3.01E-07	1.58E-06	3.34E-07
^{79}Kr	1.99E-14	5.61E-14	1.47E-08	1.30E-07	1.48E-08
^{80}Kr	2.98E-16	8.58E-13	1.21E-06	1.19E-05	1.10E-06
^{81}Kr	6.98E-21	3.15E-15	4.45E-09	6.03E-08	3.81E-09

Table 3—Continued

Species	Weak	WS6.8s	WS4.8s	WS1.0s	Strong
^{82}Kr	2.07E-24	8.06E-13	7.96E-07	1.00E-05	4.83E-07
^{83}Kr	1.24E-28	6.99E-16	4.89E-10	8.42E-09	2.80E-10
^{84}Kr	3.48E-31	9.52E-14	4.25E-08	6.53E-07	1.51E-08
^{85}Kr	9.60E-36	1.00E-17	2.67E-12	5.89E-11	9.08E-13
^{86}Kr	3.23E-38	4.04E-16	1.08E-10	2.15E-09	2.32E-11
^{87}Kr	7.94E-46	2.30E-24	4.89E-19	2.83E-17	1.00E-19

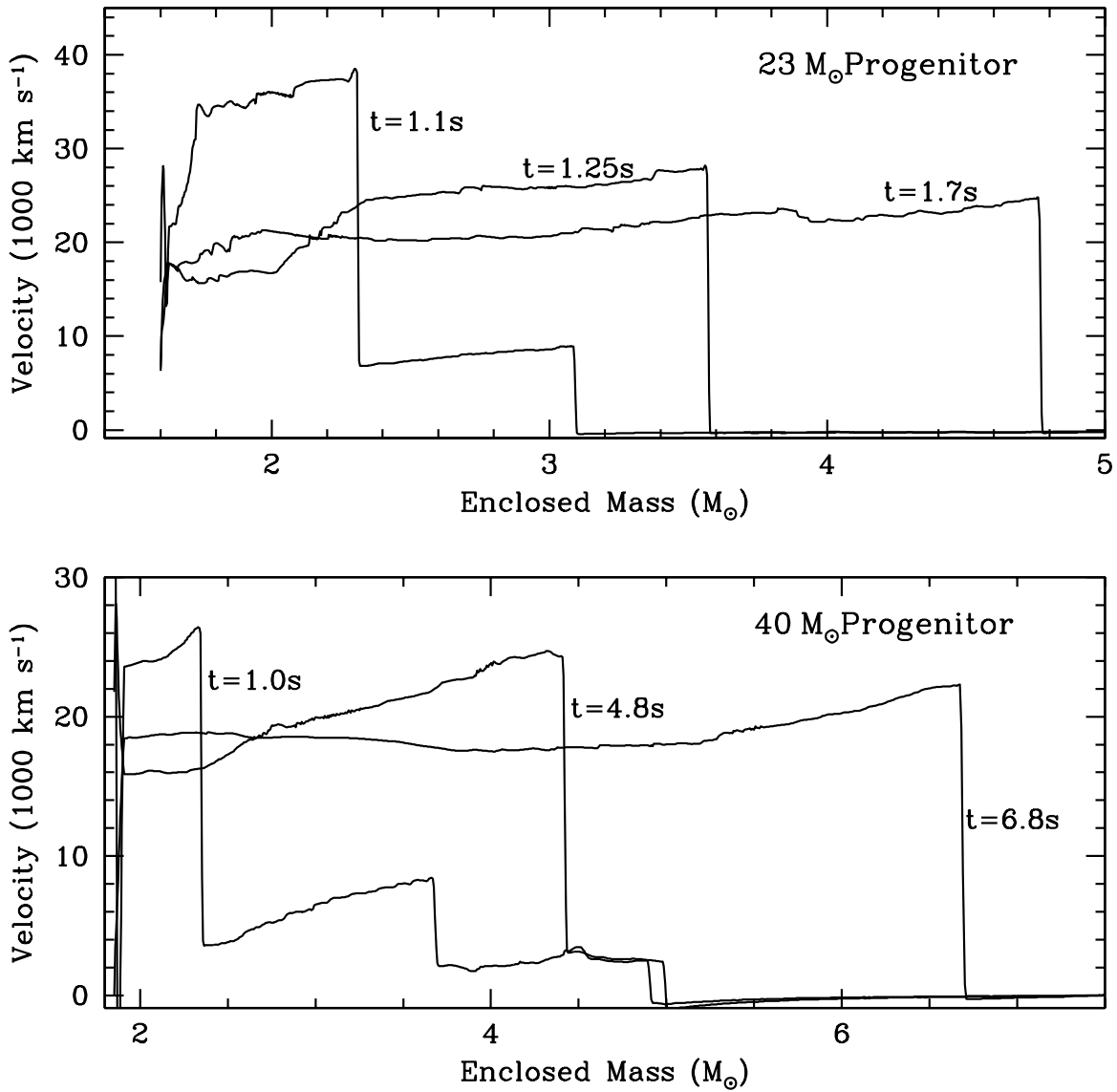


Fig. 1.— Velocity versus enclosed mass for the $23 M_\odot$ (top) and $40 M_\odot$ (bottom) progenitor with strong explosion energies ($14,15 \times 10^{51} \text{ erg}$ for the $23 M_\odot, 40 M_\odot$ progenitors). Note that the peak velocities as the shock reaches the edge of the star still exceed $20,000 \text{ km s}^{-1}$.

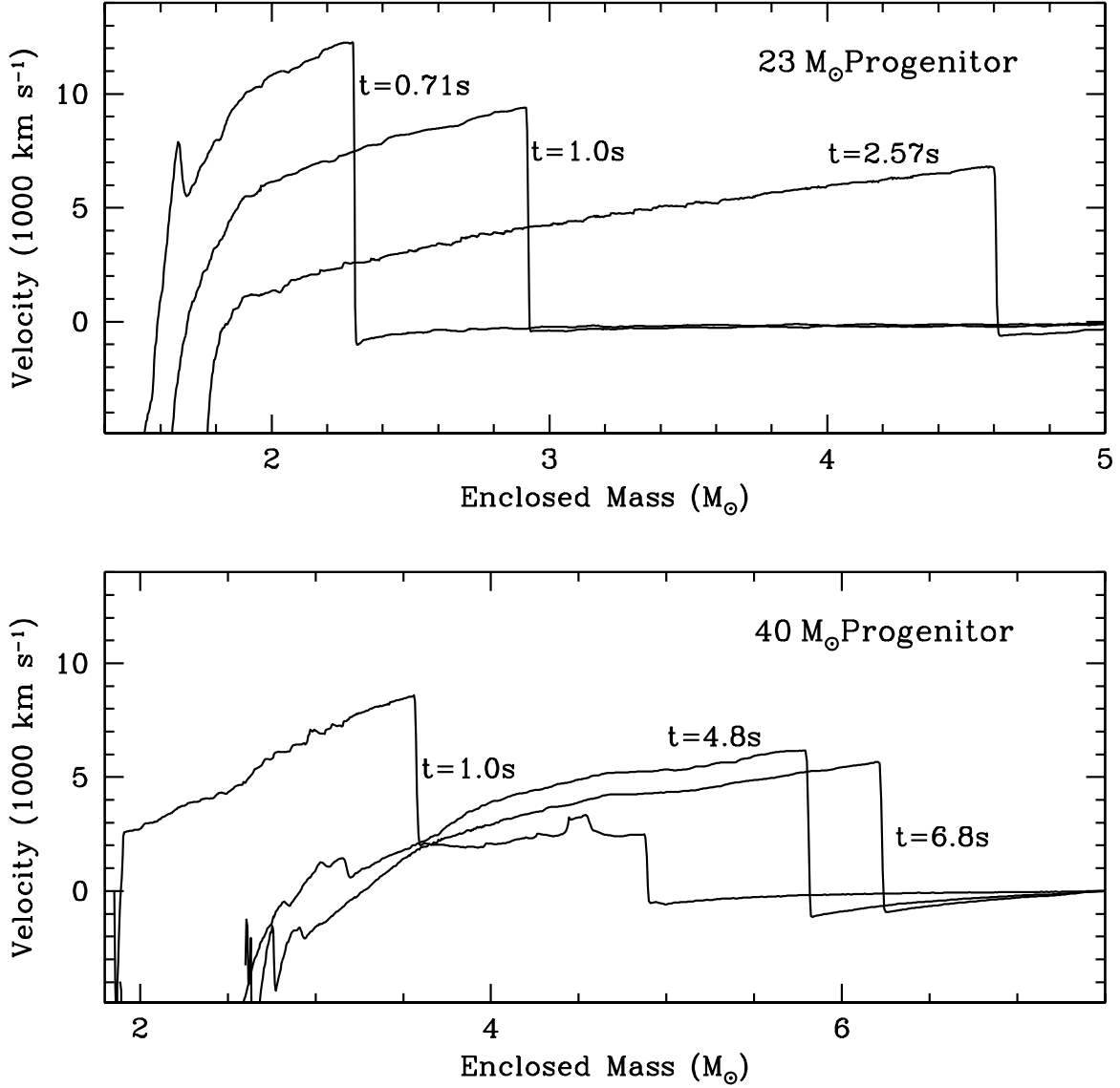


Fig. 2.— Velocity versus enclosed mass for the $23 M_{\odot}$ (top) and $40 M_{\odot}$ (bottom) progenitor with weak explosion energies ($0.25, 0.1 \times 10^{51}$ erg for the $23 M_{\odot}, 40 M_{\odot}$ progenitors). These correspond to the 23weak and 40weak simulations. We show the velocities for 3 snapshot times, corresponding to the time at which we take these models and introduce a new explosion: from left to right, we have the initial conditions for models 23WS0.7, 23WS1.0, 23WS2.6 (top panel) and models 40WS1.0, 40WS4.8, 40WS6.8 (bottom panel).

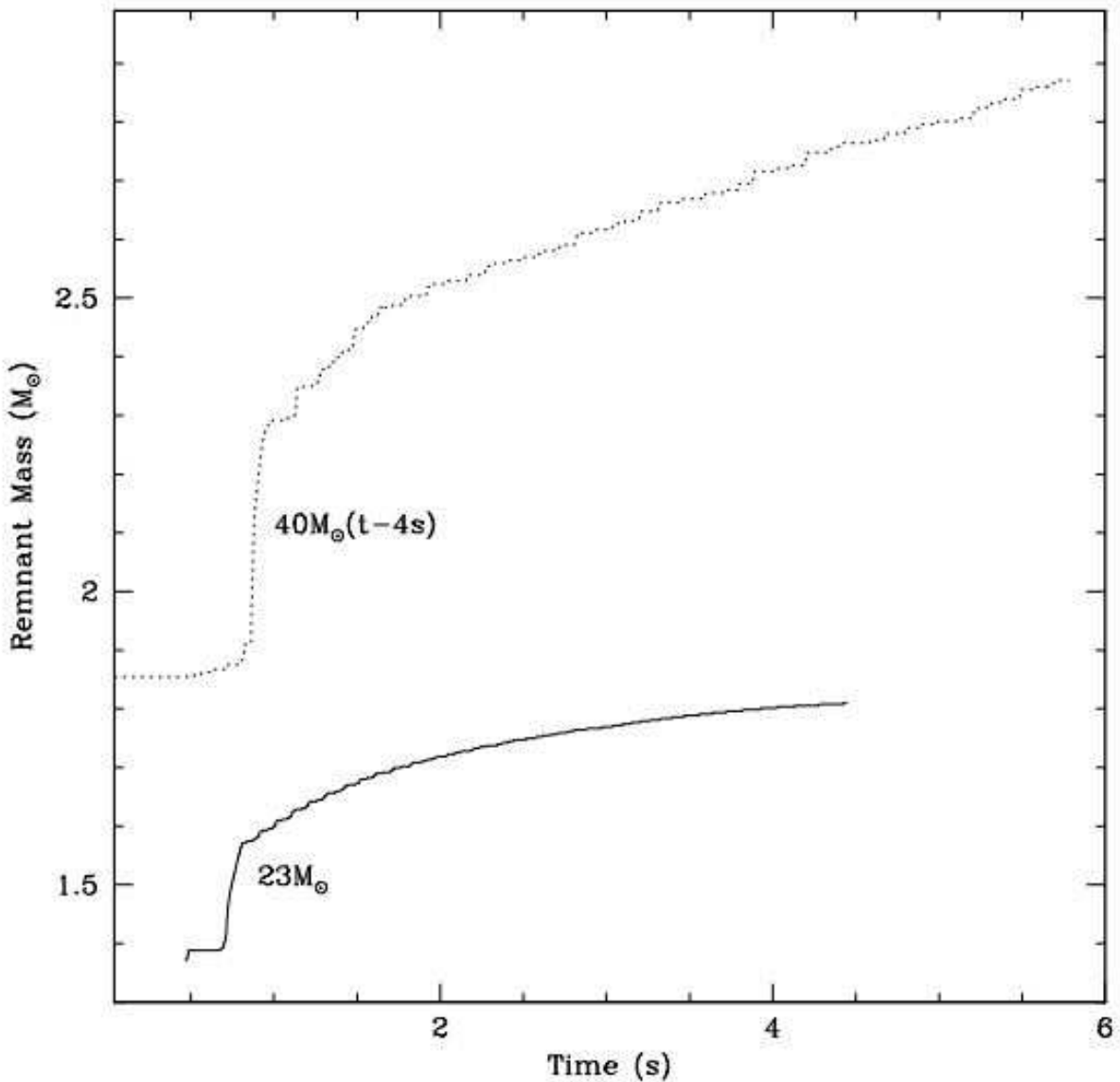


Fig. 3.— Mass of the compact remnant as a function of time for weak explosions of the $23 M_\odot$ (solid) and $40 M_\odot$ (dotted) stars. This is the mass of matter actually added to the compact remnant. The total amount of mass bound to the remnant (that will ultimately accrete onto the remnant) is much larger.

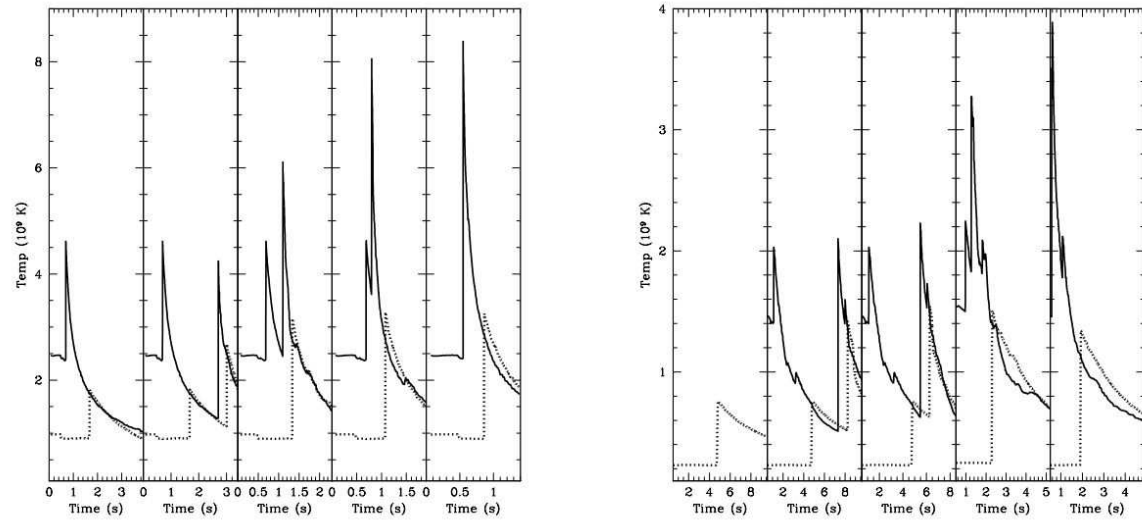


Fig. 4.— Temperature versus time for 2 mass zones for all our models. Figure 4a corresponds to the $23 M_{\odot}$ models: from left to right, model 23weak, 23WS0.7, 23WS1.0, 23WS2.6, 23strong. Figure 4b corresponds to the $40 M_{\odot}$ models: from left to right, model 40weak, 40WS1.0, 40WS4.8, 40WS6.8, 40strong. Note that the highest temperatures are achieved with a single shock. The weak shock moves the material outward, leading to lower peak temperatures when the strong shock ultimately strikes the material. Hence we expect considerably less nuclear burning in the models with long delays.

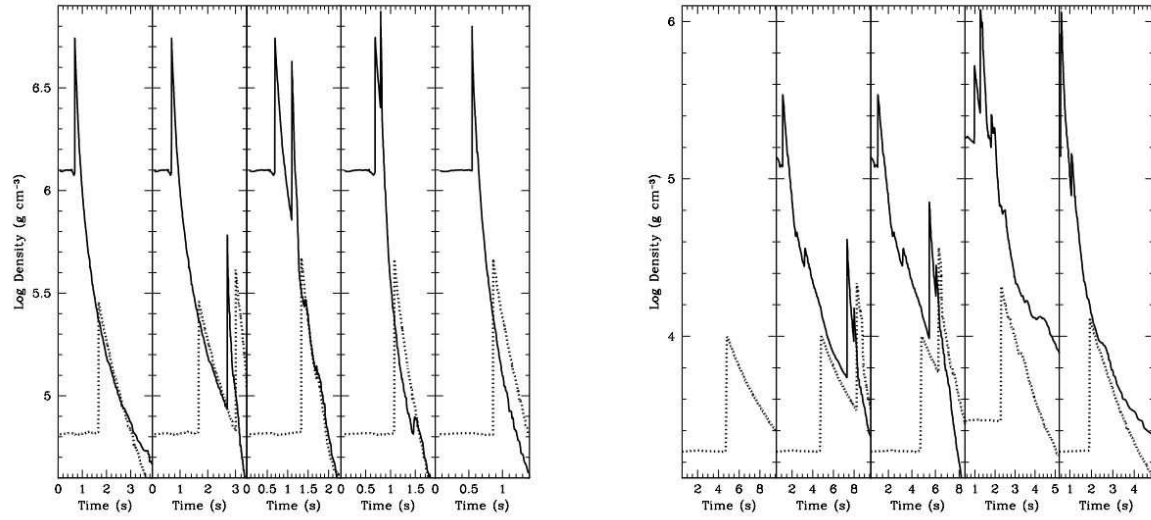


Fig. 5.— Density versus time for 2 mass zones for all our models. Figure 4a corresponds to the $23 M_{\odot}$ models: from left to right, model 23weak, 23WS0.7, 23WS1.0, 23WS2.6, 23strong. Figure 4b corresponds to the $40 M_{\odot}$ models: from left to right, model 40weak, 40WS1.0, 40WS4.8, 40WS6.8, 40strong. Note that because the density jump is insensitive to the density or strength of the shock (as long as it is a strong shock), the density of double shocked material can actually be higher in the case of a short delay. By altering both the temperature and density evolution with the delayed explosions, we are altering the yields for these models.

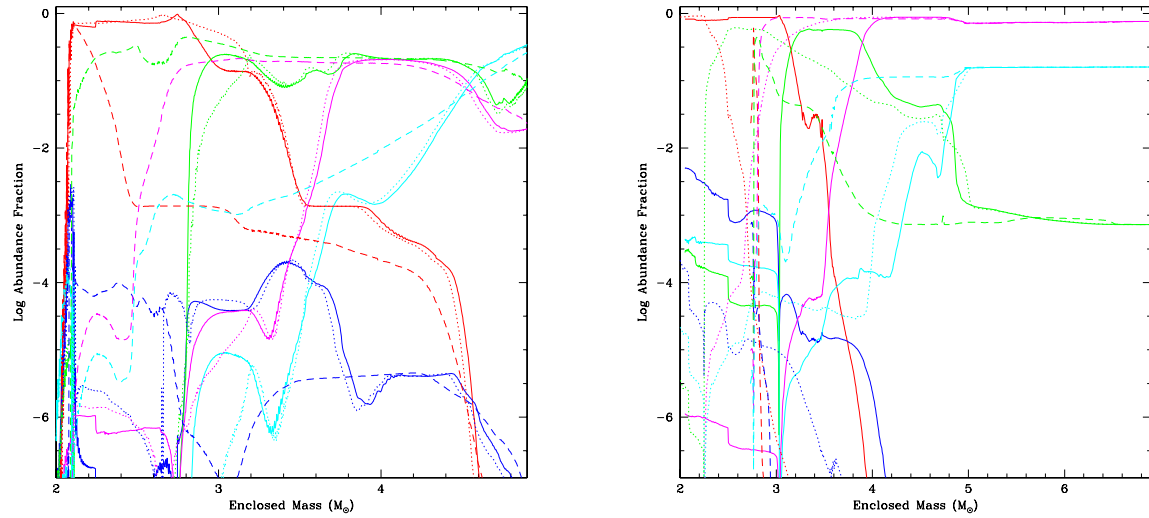


Fig. 6.— Fractional abundance versus enclosed mass for 6 of our models: panel (a) - 23strong (solid), 23WS1.0 (dotted), 23WS2.6 (dashed) and panel (b) - 40strong (solid), 40WS1.0 (dotted), 40WS4.8 (dashed). The colors denote different abundances prior to decay: ^{56}Ni (red), ^{44}Ti (blue), ^{28}Si (green), ^{16}O (magenta), ^{12}C (cyan). Note that there are zones where the ^{44}Ti yield exceeds that of the ^{56}Ni . Also note that nearly all of the He in these stars is burned into heavier elements.

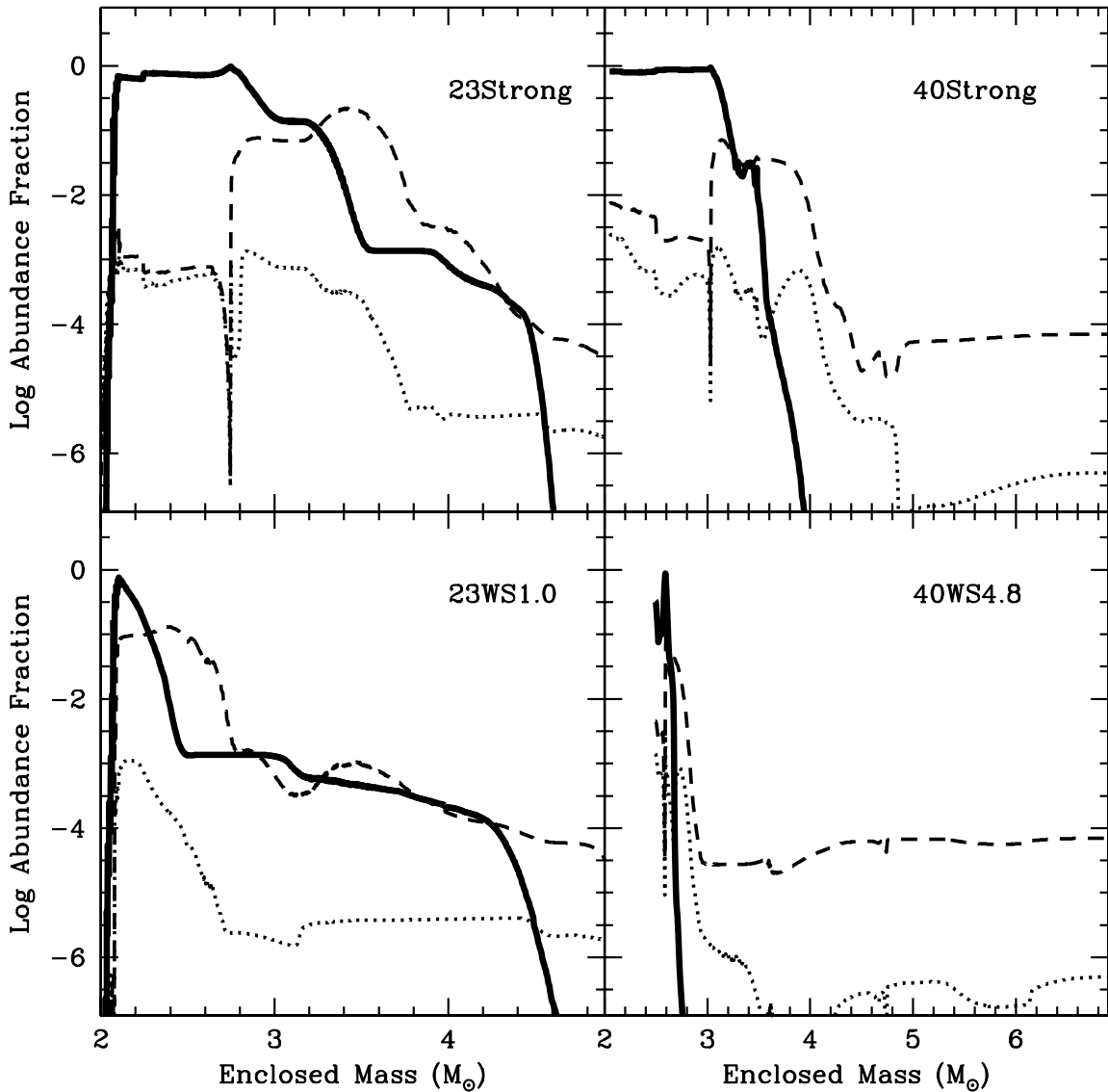


Fig. 7.— Abundance fractions of the stable calcium (dashed), titanium (dotted) and ^{56}Fe (solid) versus enclosed mass for 4 of our explosion models: 23Strong, 23WS1.0, 40Strong, 40WS4.8. The production site of the iron is most centrally condensed, followed by titanium and then calcium. For strong explosions without delay, a large fraction of the star is converted into heavy elements. With long delays, the ejecta of these heavy elements is confined to the lowest layer of ejected material.

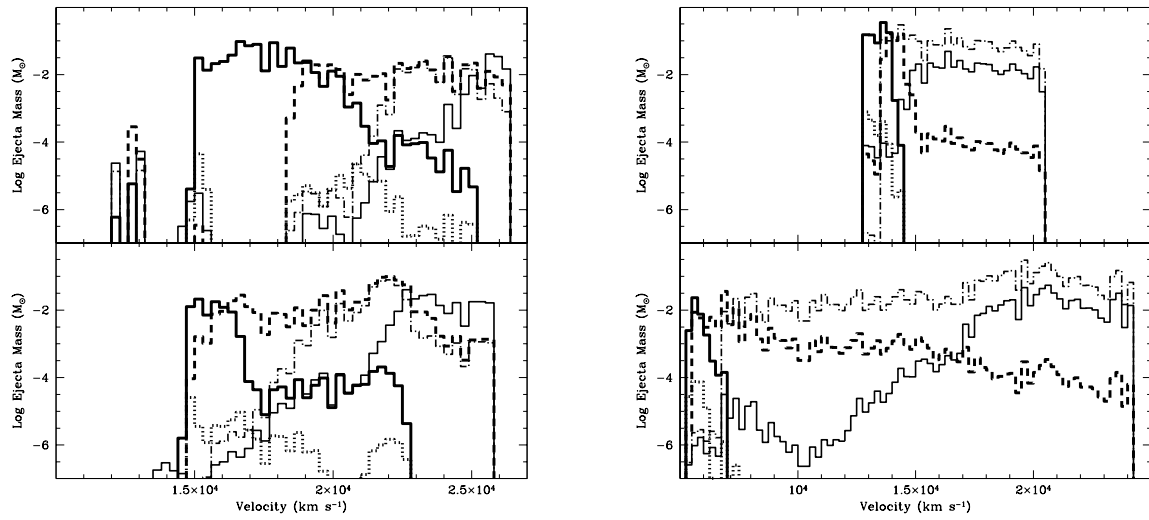


Fig. 8.— Histogram of the mass distribution (in solar masses per bin) in velocity space for ^{56}Ni (thick solid), ^{44}Ti (dotted), ^{28}Si (dashed), ^{16}O (dot-dashed), and ^{12}C (thin solid). The left panels show the results from the $23 M_{\odot}$ models (top - 23strong, bottom 23WS1.0). The right panels show the results from the $40 M_{\odot}$ models (top - 40strong, bottom 40WS1.0). No obvious trends appear and this distribution is far more dependent upon the supernova asymmetry than are the nucleosynthetic yields.